GRASPING AND MANIPULATION USING MULTIFINGERED ROBOT HANDS

by

Richard M. Murray and S. Shankar Sastry

Memorandum No. UCB/ERL M90/24

27 March 1990

GRASPING AND MANIPULATION USING MULTIFINGERED ROBOT HANDS

by

Richard M. Murray and S. Shankar Sastry

Memorandum No. UCB/ERL M90/24

27 March 1990

ELECTRONICS RESEARCH LABORATORY

College of Engineering
University of California, Berkeley
94720

GRASPING AND MANIPULATION USING MULTIFINGERED ROBOT HANDS

by

Richard M. Murray and S. Shankar Sastry

Memorandum No. UCB/ERL M90/24

27 March 1990

ELECTRONICS RESEARCH LABORATORY

College of Engineering
University of California, Berkeley
94720

Grasping and Manipulation using Multifingered Robot Hands

Richard M. Murray[1]
S. Shankar Sastry[2]

Electronics Research Laboratory
Department of Electrical Engineering and Computer Science
University of California Berkeley, CA 94610

Originally published in:

AMS Short Course Lecture Notes
Mathematical Questions in Robotics
Louisville, Kentucky Jan. 16–17, 1990

[1]Supported in part by an IBM Manufacturing Fellowship
[2]Supported in part by NSF-PYI grant DMC84-51129

Contents

Notation

G	grasp map; maps contact forces to object forces
J	hand Jacobian; maps joint velocities to contact velocities
$\mathcal{N}(A)$	null space of the matrix A
$\mathcal{R}(A)$	range space of the matrix A
$\mathcal{S}(\omega)$	skew symmetric matrix associated with ω; defined by $\mathcal{S}(\omega)a = \omega \times a$ for all $a \in \mathbf{R}$; $\mathcal{S}(\omega) \in se(3)$
$SE(3)$	special Euclidean group; rigid motions
$se(3)$	$T_eSE(3)$; Lie algebra of $SE(3)$; generalized velocity
$SO(3)$	special orthogonal group; rotation matrices
$so(3)$	$T_eSO(3)$; Lie algebra of $SO(3)$; rotational velocity
$[f,g]$	Lie bracket between two vector fields; in coordinates $[f,g] = \frac{\partial g}{\partial x} f - \frac{\partial f}{\partial x} g$

k	number of fingers
m_i	number of forces exerted by the i^{th} contact
m	total number of grasping constraints
n_i	number of degrees of freedom of the i^{th} finger
n	total number of degrees of freedom for the hand

Chapter 1

Introduction

In these notes we give the reader a feel for the mathematical problems involved in describing grasping and fine motion manipulation of objects with multifingered robot hands. Multifingered robot hands can be thought of as several robots (fingers) on a common base (palm) cooperatively manipulating an object. It is clear that positioning an object in space, namely specifying its position and orientation needs 6 degrees of freedom. However, dextrously manipulating objects requires far more degrees of freedom especially in the execution of tasks involving picking up an object, regrasping it and using the object. It is here that the study of multifingered hands is important. The study of multifingered hands has a long history not just in the context of robotics but also in the context of prosthesis.

In Chapter 2, we set down a brief discussion of the kinematics of a single rigid body, followed by a study of contacts and the kinematics of rolling. Rolling is an especially important way in which finger tips move over the surface of an object in order both to reposition and regrasp the object. In Section 2.4 we study the kinematics of a multifingered hand in terms of the kinematics of the individual fingers. Finally, we define grasp stability and the manipulability of grasps. The appendix contains a derivation of the contact equations in terms of the metric tensor and connection form of the surfaces in contact at the finger tip and object.

In Chapter 3, we develop the dynamics of multifingered hands by aggregating the dynamics of individual fingers with the dynamics of the grasped object and the kinematic equations of contact. In Section 3.3 we describe a few different control techniques to follow a specified trajectory for the body and the grasp forces exerted on it.

In Chapter 4, we axiomatize the process of regrasping an object by rolling the finger tips on the surface of the object. We show how the problem of finding geodesics for singular or Carnot-Caratheodory metrics is useful in steering the finger tips from one grasp to another. We conclude with some open problems.

The discussion of this paper is a summary of our own work and that of others, notably those at Harvard, in the last few years in this area. Detailed references to these appear in the body of the notes.

Chapter 2

Kinematics and Statics

This chapter provides a brief introduction to grasping and the notation used in this paper. We derive the basic velocity and force transformations for both fixed and rolling contacts. For a more complete discussion of the kinematics of grasping see Kerr [5] and Montana [12].

2.1 Rigid body kinematics

A rigid motion of an object is a motion which preserves distance and orientation. Every such rigid motion can be represented by a rotation followed by a translation. Letting $SO(3)$ represent the group of all proper 3×3 rotation matrices and $\mathbb{R}$ denote the real numbers, we can represent a rigid motion by the pair $(R, p) \in SO(3) \times \mathbb{R}^3$. We define $SE(3) = SO(3) \times \mathbb{R}^3$ to be the set of all rigid motions and note that $SE(3)$ is a manifold of dimension 6 as well as a group. It may be verified that $SE(3)$ is a Lie group.

The configuration of a rigid body with respect to some identity configuration is described by an element $g \in SE(3)$. g acting on a point attached to the body defines the new location of the point relative to its identity configuration. If $q \in \mathbb{R}^3$ is a point on the body relative to some base (world) reference frame, then the location of q with respect to that basis after the body undergoes a rigid motion g is

$$g(q) = Rq + p \tag{2.1}$$

where R and p are represented in the same basis as q. This action is shown pictorially in Figure 2.1. We refer to the absolute coordinates as the *world* or *base coordinates* and the coordinates of a point on the object relative to the identity configuration as the *body coordinates.*

An object trajectory is described by a time parameterized curve, $g(t) \in SE(3)$. The velocity of an object is a tangent vector at g, so $\dot{g} \in T_gSE(3)$. $\dot{g}$ also acts on points in $\mathbb{R}^3$, giving a velocity vector $\dot{g}(q) \in \mathbb{R}^3$. Since $SE(3)$ is

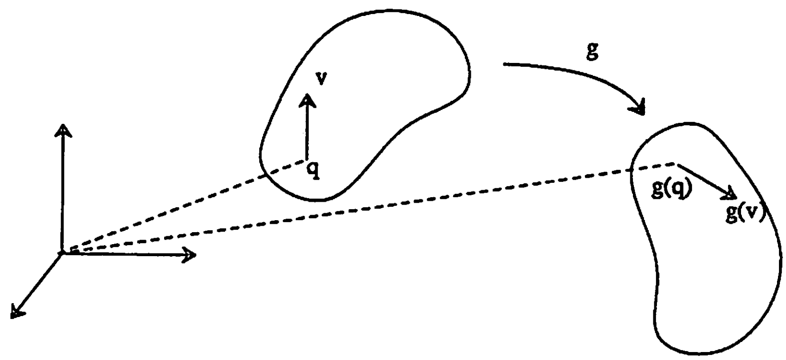

Figure 2.1: Rigid motion

a Lie group, we can associate each element of $T_gSE(3)$ with the Lie algebra $se(3) \approx T_eSE(3)$ where e is the identity element. An element $\xi \in se(3)$ can be represented as a skew symmetric matrix, $\mathcal{S} \in so(3)$ and a vector $v \in \mathbb{R}^3$. Furthermore, any skew symmetric matrix has the form:

$$\mathcal{S} = \begin{bmatrix} 0 & -\omega_z & \omega_y \\ \omega_z & 0 & -\omega_x \\ -\omega_y & \omega_x & 0 \end{bmatrix} \tag{2.2}$$

and hence we will often write $\mathcal{S}(\omega) \in so(3)$ to be the skew symmetric matrix associated with $\omega \in \mathbb{R}^3$. Note that $\mathcal{S}(\omega)q = \omega \times q$.

There are two ways to map $T_gSE(3)$ to $T_eSE(3)$ — left and right translation. The usual method is to use left translation, $L_{g^{-1}}$, where $L_g h = g \circ h$. The tangent map of $L_{g^{-1}}$ maps $T_gSE(3)$ to $T_eSE(3)$ and when applied to $\dot{g}$, the resulting map, $T_{g^{-1}}(L_{g^{-1}})\dot{g}$, takes a point in body coordinates to the velocity in body coordinates. For our purposes it is more natural to use the velocity of the point in world coordinates. This can be accomplished by using right translation and the resulting map takes a point in world coordinates to a velocity in world coordinates. Formally, we define the generalized velocity, $\xi \in T_eSE(3)$, in terms of $\dot{g} \in T_gSE(3)$ as

$$\xi = \dot{g}g^{-1} \tag{2.3}$$

The generalized velocity ξ is also called a *twist*.

Elements of $SE(3)$ can be represented as 4×4 matrices, referred to as *homogeneous coordinates*. If $g \in SE(3)$ we write

$$g = \begin{bmatrix} R & p \\ 0 & 1 \end{bmatrix} \tag{2.4}$$

A point $q \in \mathbb{R}^3$ can be represented as a vector in $\mathbb{R}^4$ by defining $\tilde{q} = (q, 1) \in$

$\mathbb{R}^3 \times \mathbb{R}$. Using this representation, $g(q)$ becomes matrix multiplication

$$g\tilde{q} = \begin{bmatrix} R & p \\ 0 & 1 \end{bmatrix} \begin{pmatrix} q \\ 1 \end{pmatrix} = \begin{pmatrix} Rq + p \\ 1 \end{pmatrix} \tag{2.5}$$

To simplify notation we shall usually refer to $\tilde{q}$ simply as q.

The generalized velocity of a motion, in world coordinates, is

$$\xi = \dot{g}g^{-1} = \begin{bmatrix} \dot{R}R^T & \dot{p} - \dot{R}R^T p \\ 0 & 0 \end{bmatrix} \tag{2.6}$$

which can be rewritten as

$$\xi = \begin{bmatrix} \mathcal{S}(\omega) & v \\ 0 & 0 \end{bmatrix} \tag{2.7}$$

where $\omega \in \mathbb{R}^3$, $v \in \mathbb{R}^3$ and $\mathcal{S}(\omega)$ is the skew symmetric matrix generated by ω. The vector

$$\hat{\xi} = \begin{pmatrix} v \\ \omega \end{pmatrix} \tag{2.8}$$

is referred to as the *twist coordinates* of ξ and represents the rotational and linear velocity of an object as viewed in world coordinates.

2.2 Fixed contact kinematics

Traditionally, a *fixed contact* between a finger and an object is described as a mapping between forces exerted by the finger at the point of contact and the resultant forces at some reference point on the object (e.g., the center of mass). We represent the force exerted at the i^{th} contact as $\tilde{F}_{c_i} = (\tilde{f}_{c_i}, \tilde{\tau}_{c_i}) \in \mathbb{R}^6$ where $\tilde{f}_{c_i}$ is the force exerted by contact and $\tilde{\tau}_{c_i}$ is the moment. The relationship between contact force and object force has the form

$$F_o = \begin{pmatrix} f_o \\ \tau_o \end{pmatrix} = \begin{pmatrix} \tilde{f}_{c_i} \\ \tilde{\tau}_{c_i} + r_{c_i} \times \tilde{f}_{c_i} \end{pmatrix} = \begin{bmatrix} I & 0 \\ \mathcal{S}(r_{c_i}) & I \end{bmatrix} \tilde{F}_{c_i} \tag{2.9}$$

where $r_{c_i} \in \mathbb{R}^3$ is the vector between the object reference point and the contact.

Typically, a finger will not be able to exert forces in every direction; several simple contact models are used to classify common contact configurations. A *point contact* is obtained when there is no friction between the fingertip and the object. In this case, forces can only be applied in the direction normal to the surface of the object and hence we can represent the applied force as

$$\tilde{F}_{c_i} = \begin{bmatrix} n_{c_i} \\ 0 \end{bmatrix} f_{c_i} \tag{2.10}$$

where n_{c_i} is the unit vector normal to the object and $f_{c_i} \in \mathbb{R}$ is the amount of force applied by the finger in that direction.

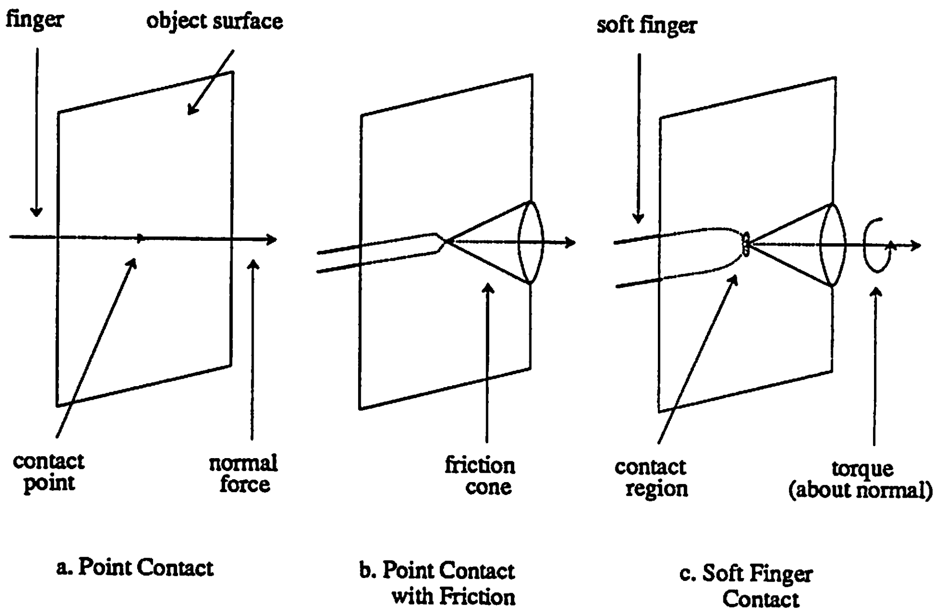

Figure 2.2: Contact types

A *point contact with friction* model is used when friction exists between the fingertip and the object, in which case forces can be exerted in any direction that is within a cone of forces about the direction of the surface normal. This cone, called the *friction cone*, is determined by the coefficient of friction. Figure 2.2b shows a point contact with friction and the resultant friction cone. This model assumes that moments cannot be applied (i.e., there is no torsional friction about the surface normal). As before, we represent the force felt by the object with respect to a basis of directions which are consistent with the friction model:

$$\tilde{F}_{c_i} = \begin{bmatrix} I \\ 0 \end{bmatrix} f_{c_i} \tag{2.11}$$

with $f_{c_i} \in \mathbb{R}^3$.

A more realistic contact model is the *soft finger* contact. Here we allow not only forces to be applied in a cone about the surface normal but also torques about that normal (see Figure 2.2c). These torques are limited by the torsional friction coefficient. Inside the relevant friction cones, this contact can be described as

$$\tilde{F}_{c_i} = \begin{bmatrix} I & 0 \\ 0 & n_{c_i} \end{bmatrix} \begin{pmatrix} f_{c_i} \\ \tau_{c_i} \end{pmatrix} \tag{2.12}$$

where $f_{c_i} \in \mathbb{R}^3$ and $\tau_{c_i} \in \mathbb{R}$.

Matrices mapping finger forces to contact force as in equations (2.10), (2.11) and (2.12) are referred to as *selection matrices* and we denote them by $B_i(x_o) \in$

$\mathbb{R}^{6\times m_i}$, where m_i is the dimension of the range of forces and moments that can be applied for a given contact type. Note their dependence on the (fixed) contact point and the orientation of the object. Each of the contact types thus can be represented as a linear map $G_i(r_{c_i}, x_o)\colon F_{c_i} \in \mathbb{R}^{m_i} \mapsto F_o$

$$G_i(r_{c_i}, x_0) = \begin{bmatrix} I & 0 \\ \mathcal{S}(r_{c_i}) & I \end{bmatrix} B_i(x_0) \tag{2.13}$$

Since r_{c_i} is a function of the object orientation, we shall usually write $G_i(r_{c_i}, x_o)$ as $G_i(x_o)$.

If we have several fingers contacting an object then the net force on the object is the sum of the forces due to each finger. The *grasp map*, $G\colon \mathbb{R}^m \to \mathbb{R}^6$, is the map between finger forces and the resultant total object force. Since each contact map is linear and forces can be superposed, we can add the individual contact maps to form G:

$$F_o = \begin{bmatrix} G_1 & \cdots & G_k \end{bmatrix} \begin{pmatrix} F_{c_1} \\ \vdots \\ F_{c_k} \end{pmatrix} = GF_c, \qquad \begin{array}{l} F_o \in \mathbb{R}^6 \\ F_c \in \mathbb{R}^{m_1} \times \mathbb{R}^{m_2} \times \ldots \times \mathbb{R}^{m_k} \end{array} \tag{2.14}$$

The null space of the grasp map corresponds to finger forces which cause no net force to be exerted on the object. We call the force on the object resulting from finger forces which lie in the null space of G, denoted $\mathcal{N}(G)$, *internal* or *null forces*. It is in part these internal forces which allow us to grip or squeeze an object.

Dual to the representation of contacts as applied force and torque, one may also represent a contact as a constraint between the relative velocity of the object and the finger. Letting v_{c_i} and ω_{c_i} represent the linear and angular velocity of the contact point and v_o and ω_o represent the object velocity,

$$\begin{pmatrix} \tilde{v}_{c_i} \\ \tilde{\omega}_{c_i} \end{pmatrix} = \begin{bmatrix} I & \mathcal{S}(r_{c_i}) \\ 0 & I \end{bmatrix} \begin{pmatrix} v_o \\ \omega_o \end{pmatrix} \tag{2.15}$$

If we define v_c to be the velocities conjugate to f_c, the forces exerted by the fingers, it follows that

$$\begin{pmatrix} v_c \\ \omega_c \end{pmatrix} = G^T \begin{pmatrix} v_o \\ \omega_o \end{pmatrix} \tag{2.16}$$

This relationship between object velocity and finger velocities can also be derived in a more general setting using the principle of virtual work.

Example

Consider a simple two-fingered planar hand as shown in Figure 2.3. Since we are in the plane, the grasp matrix maps finger forces into x and y forces, and a

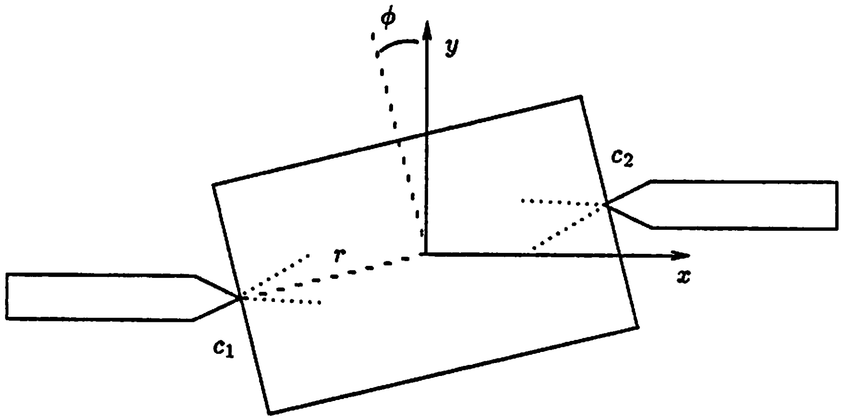

Figure 2.3: Planar two fingered grasp

torque perpendicular to the xy plane. If we assume that the contacts are point contacts with friction,

$$G_i(x,y,\phi) = \begin{bmatrix} I & 0 \\ \mathcal{S}\begin{pmatrix} \pm r\cos\phi \\ \pm r\sin\phi \\ 0 \end{pmatrix} & I \end{bmatrix} \begin{bmatrix} 1 & 0 \\ 0 & 1 \\ 0 & 0 \\ 0 & 0 \\ 0 & 0 \\ 0 & 0 \end{bmatrix} \qquad (2.17)$$

and the planar grasp map for Figure 2.3 is

$$G(x,y,\phi) = \underbrace{\begin{bmatrix} 1 & 0 & 1 & 0 \\ 0 & 1 & 0 & 1 \\ r\sin(\phi) & -r\cos(\phi) & -r\sin(\phi) & r\cos(\phi) \end{bmatrix}}_{G_1 \qquad\qquad G_2} \qquad (2.18)$$

where all forces are measured with respect to the xy coordinates shown in the figure.

Equation (2.18) shows that x and y forces from the fingers cause the same x and y forces to be exerted on the object as well as a torque that is dependent on the orientation of the object. The null space of this map is spanned by the vector

$$\begin{pmatrix} \cos\phi \\ \sin\phi \\ -\cos\phi \\ -\sin\phi \end{pmatrix} \qquad (2.19)$$

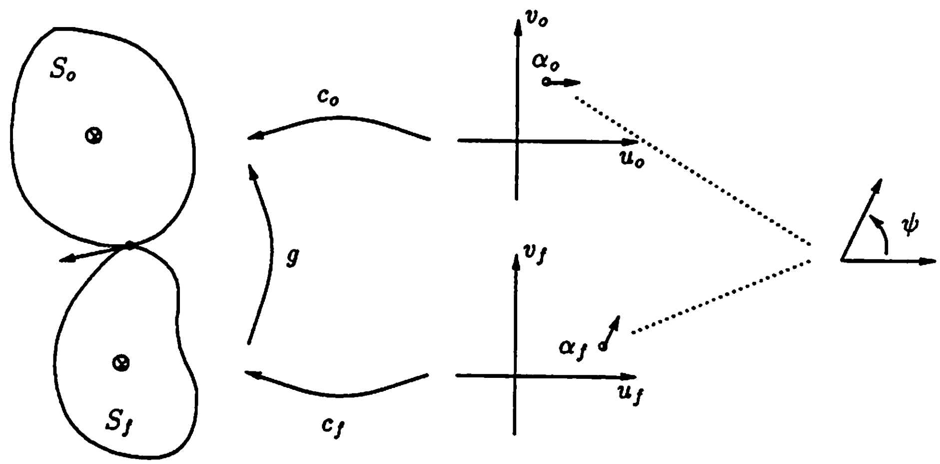

Figure 2.4: Parameterization of rolling contacts

which corresponds to forces applied along the line connecting the two fingertips. Finger forces applied along this line will cause no net force on the object.

2.3 Rolling contact kinematics

Most real world grasping situations involve moving rather than fixed contacts. Human fingers and many robotic fingers are actually surfaces and manipulation of an object by a set of fingers involves rolling of the fingers along the object surface. In this section we derive the kinematic equations for one object rolling against another.

Consider two objects, S_o and S_f in $\mathbf{R}^3$ which are touching at a point. We will restrict ourselves to the case where motion is contained in a single coordinate chart for each object. Let (c_o, U_o) and (c_f, U_f) be charts for the two surfaces and $\alpha_o = (u_o, v_o) \in U_o$ and $\alpha_f = (u_f, v_f) \in U_f$ be local coordinates. We will assume that c_o and c_f are orthogonal representations of the surface.[1] Furthermore, we let ψ represent the relative orientation of the tangent planes at the point of contact (see Figure 2.4). We call $\eta = (\alpha_o, \alpha_f, \psi)$ the *contact coordinates.*

Let $g \in SE(3)$ describe the relative position and orientation of S_f with respect to S_o. We wish to study the relationship between g and the local contact coordinates. To do so we assume that $g \in W \subset SE(3)$ where W is the set of all relative positions for which the two objects remain in contact.

We begin by writing the algebraic equations that η must satisfy. At any

[1] A surface representation $c: (u, v) \rightarrow R^3$ is orthogonal if $\frac{\partial c}{\partial u}$ and $\frac{\partial c}{\partial v}$ are orthogonal. Such a representation can always be constructed for a regular surface in a given coordinate chart.

point of contact the location of the contact in space must agree for both objects

$$g \circ c_f(\alpha_f) = c_o(\alpha_o) \tag{2.20}$$

Furthermore, the tangent planes must coincide and hence the outward surface normals $n_o : S_o \rightarrow S^2 \subset \mathbb{R}^3$ and $n_f : S_f \rightarrow S^2 \subset \mathbb{R}^3$ must also agree. Letting $R \in SO(3)$ be the rotational component of g

$$Rn_f(\alpha_f) = -n_o(\alpha_o) \tag{2.21}$$

Finally, we define the angle between the tangent planes as the unique angle $\psi \in [0, 2\pi)$ such that

$$R\frac{\partial c_f}{\partial \alpha_f} M_f^{-1} R_\psi = \frac{\partial c_o}{\partial \alpha_o} M_o^{-1} \tag{2.22}$$

where

$$M_i = \begin{bmatrix} \|\frac{\partial c_i}{\partial u_i}\| & 0 \\ 0 & \|\frac{\partial c_i}{\partial v_i}\| \end{bmatrix} \tag{2.23}$$

insures that the columns of $\frac{\partial c}{\partial \alpha}$ are unit length and

$$R_\psi = \begin{bmatrix} \cos\psi & -\sin\psi \\ -\sin\psi & -\cos\psi \end{bmatrix} \tag{2.24}$$

converts α_o coordinates to the equivalent α_f coordinates at the point of contact. Since the normals are in opposite directions, R_ψ acts by negating the y coordinate and rotating by an angle ψ. Note that $R_\psi = R_\psi^T = R_\psi^{-1}$.

Proposition 1 *There is a smooth local bijection between η and $g \subset W$ if and only if*

$$\frac{\partial n_o}{\partial \alpha_o} M_o^{-1} + R\frac{\partial n_f}{\partial \alpha_f} M_f^{-1} R_\psi$$

is full rank

Proof. Functionally, equations (2.20) through (2.22) are of the form $h(g, \eta) = 0$. It is therefore sufficient (and necessary) to show that $\frac{\partial h}{\partial \eta}$ spans the allowable velocity space, TW. Since ψ can be defined directly, we omit the ψ coordinate and consider the dependence on $\alpha = (\alpha_o, \alpha_f)$,

$$h(g,\alpha) = \begin{pmatrix} c_o(\alpha_o) - gc_f(\alpha_f) \\ n_o(\alpha_o) + Rn_f(\alpha_f) \end{pmatrix} \tag{2.25}$$

$$\frac{\partial h}{\partial \alpha}(g,\alpha) = \begin{pmatrix} \frac{\partial c_o(\alpha_o)}{\partial \alpha_o} & -R\frac{\partial c_f(\alpha_f)}{\partial \alpha_f} \\ \frac{\partial n_o(\alpha_o)}{\partial \alpha_o} & R\frac{\partial n_f(\alpha_f)}{\partial \alpha_f} \end{pmatrix} \tag{2.26}$$

First we show that the span of the rows of $\frac{\partial h}{\partial \alpha}$ does not contain either $(n_o, 0)$ or $(0, n_o)$, corresponding to translation and rotation about n_o. $(0, n_o)$ is spanned directly by $d\psi$ and $(n_o, 0)$ should not belong to the row span of $\frac{\partial h}{\partial \alpha}$ because motion in the n_o direction is not contained in TW. Since the range of $\frac{\partial c_o}{\partial \alpha_o}$ and $\frac{\partial c_f}{\partial \alpha_f}$ define the tangent plane and the n_i's have unit magnitude and using equation (2.21), we find

$$\begin{pmatrix} n_o \\ 0 \end{pmatrix}^T \frac{\partial h}{\partial \alpha} = \begin{bmatrix} n_o^T \frac{\partial c_o}{\partial \alpha_o} & n_f^T R^T R \frac{\partial c_f}{\partial \alpha_f} \end{bmatrix} = 0 \tag{2.27}$$

$$\begin{pmatrix} 0 \\ n_o \end{pmatrix}^T \frac{\partial h}{\partial \alpha} = \begin{bmatrix} n_o^T \frac{\partial n_o}{\partial \alpha_o} & n_f^T R^T R \frac{\partial n_f}{\partial \alpha_f} \end{bmatrix} = 0 \tag{2.28}$$

Next we examine the conditions under which $\frac{\partial h}{\partial \alpha}$ loses rank. Plugging equation (2.22) into equation (2.26), $\frac{\partial h}{\partial \alpha}$ can only lose rank when $\frac{\partial c_f}{\partial \alpha_f} = M_f^{-1} R_\psi M_o \frac{\partial c_o}{\partial \alpha_o}$, so $\frac{\partial h}{\partial \alpha}$ is full rank if and only if

$$\frac{\partial n_o}{\partial \alpha_o} M_o^{-1} + R \frac{\partial n_f}{\partial \alpha_f} M_f^{-1} R_\psi \tag{2.29}$$

is full rank. □

Proceeding along the lines of the proof given above, the differential relationship between η and g can be derived (see appendix at end of this chapter). It is convenient to make use of the *normalized gauss frame* defined on each surface

$$\begin{bmatrix} x_i & y_i & z_i \end{bmatrix} = \begin{bmatrix} \frac{\partial c_i}{\partial \alpha_i} M_i^{-1} & n_i \end{bmatrix} \tag{2.30}$$

If we do not allow the fingers to slide on the object (soft finger contacts) then the motion of the contacts, $\dot{\eta}$, as a function of the relative motion, (ω, v), is given by

$$\begin{aligned} \dot{\alpha}_o &= M_o^{-1}(K_o + \tilde{K}_f)^{-1}\omega_t \\ \dot{\alpha}_f &= M_f^{-1} R_\psi (K_o + \tilde{K}_f)^{-1}\omega_t \\ \dot{\psi} &= T_o M_o \dot{\alpha}_o + T_f M_f \dot{\alpha}_f \end{aligned} \tag{2.31}$$

where

$$\omega_t = \begin{bmatrix} x_o^T \\ y_o^T \end{bmatrix} n_o \times \omega \tag{2.32}$$

$$K_o = \begin{bmatrix} x_o^T \\ y_o^T \end{bmatrix} \frac{\partial n_o}{\partial \alpha_o} M_o^{-1} \tag{2.33}$$

$$\tilde{K}_f = R_\psi \begin{bmatrix} x_f^T \\ y_f^T \end{bmatrix} \frac{\partial n_f}{\partial \alpha_f} M_f^{-1} R_\psi \tag{2.34}$$

$$T_o = y_o^T \frac{\partial x_o}{\partial \alpha_o} M_o^{-1} \tag{2.35}$$

$$T_f = y_f^T \frac{\partial x_f}{\partial \alpha_f} M_f^{-1} \tag{2.36}$$

$(K_o + \tilde{K}_f)$ is called the *relative curvature* [12]. From equations (2.22) and (2.29) we see that the relative curvature is invertible precisely when $\frac{\partial h}{\partial \eta}$ is onto TW. We shall assume that all manipulation occurs in an open set on which the relative curvature is invertible.

We can now describe the kinematics for rolling contact—the relationship between the object velocities and a set of finger velocities. This situation is identical to that given for fixed contacts except that the vector r_{c_i} between the object reference frame and the i^{th} contact point is now a function of η as well as the object orientation. But η is a continuous function of $g = x_o^{-1} x_{f_i}$ so we have

$$F_o = G(x_o, x_f) F_c \tag{2.37}$$

where $x_f = (x_{f_1}, \cdots, x_{f_k})$ is the position and orientation of the fingers and $F_c \in \mathbb{R}^{n_f} \times \cdots \times \mathbb{R}^{n_k}$ is the force exerted by the fingers at the contact point. As before, G is composed of matrices of the form

$$G_i(x_o, x_f) = \begin{bmatrix} I & 0 \\ \mathcal{S}(r_{c_i}) & I \end{bmatrix} B_i(x_o, x_f) \tag{2.38}$$

The velocity relationship can again be derived from the principle of virtual work or algebraically to determine

$$\begin{pmatrix} v_c \\ \omega_c \end{pmatrix} = G^T(x_o, x_f) \begin{pmatrix} v_o \\ \omega_o \end{pmatrix} \tag{2.39}$$

Examples

To illustrate the form of the contact equations, we consider two examples—a sphere rolling on a plane and a sphere rolling on another sphere. The local coordinates of the plane are choosen to be $c_o(u, v) = (u, v, 0)$. The sphere requires multiple coordinate charts to describe the entire surface, so we shall restrict ourself to the chart

$$c_f(u, v) = (\rho \cos u \cos v, -\rho \cos u \sin v, \rho \sin u) \tag{2.40}$$

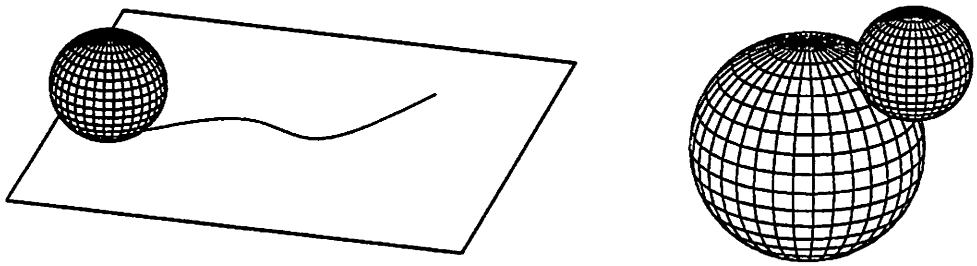

Figure 2.5: Spherical finger rolling on a plane and on another sphere. The finger is only allowed to roll on the object and not slip or twist.

where ρ is the radius of the sphere and $-\pi/2 < u < \pi/2$, $-\pi < v < \pi$. The curvature, torsion and metric tensors are easily calculated to be

$$\begin{aligned}
K_o &= \begin{bmatrix} 0 & 0 \\ 0 & 0 \end{bmatrix} & K_f &= \begin{bmatrix} 1/\rho & 0 \\ 0 & 1/\rho \end{bmatrix} \\
M_o &= \begin{bmatrix} 1 & 0 \\ 0 & 1 \end{bmatrix} & M_f &= \begin{bmatrix} \rho & 0 \\ 0 & \rho\cos u \end{bmatrix} \\
T_o &= \begin{bmatrix} 0 & 0 \end{bmatrix} & T_f &= \begin{bmatrix} 0 & -1/\rho\tan u \end{bmatrix}
\end{aligned} \tag{2.41}$$

Consider first a spherical finger of radius ρ rolling on a plane. The equations governing the evolution of the contact point are

$$\begin{aligned}
\dot{u}_f &= \omega_1 \\
\dot{v}_f &= \sec u_f\, \omega_2 \\
\dot{u}_o &= \rho\cos\psi\, \omega_1 - \rho\sin\psi\, \omega_2 \\
\dot{v}_o &= -\rho\sin\psi\, \omega_1 - \rho\cos\psi\, \omega_2 \\
\dot{\psi} &= -\tan u_f\, \omega_2
\end{aligned} \tag{2.42}$$

where $\omega_t = (\omega_1, \omega_2)$. If our object is a sphere of unit radius instead of a plane, the contact equations become

$$\begin{aligned}
\dot{u}_f &= \tfrac{1}{1+\rho}\, \omega_1 \\
\dot{v}_f &= \tfrac{1}{1+\rho} \sec u_f\, \omega_2 \\
\dot{u}_o &= \tfrac{\rho}{1+\rho} \cos\psi\, \omega_1 - \tfrac{\rho}{1+\rho} \sin\psi\, \omega_2 \\
\dot{v}_o &= -\tfrac{\rho}{1+\rho} \sin\psi \sec u_o\, \omega_1 - \tfrac{\rho}{1+\rho} \cos\psi \sec u_o\, \omega_2 \\
\dot{\psi} &= \tfrac{\rho}{1+\rho} \sin\psi \tan u_o\, \omega_1 + \tfrac{\rho}{1+\rho}(\cos\psi \tan u_o - 1rho\ \tan u_f)\, \omega_2
\end{aligned} \tag{2.43}$$

2.4 Finger Kinematics

Up to this point we have assumed that the fingers of the hand are points or surfaces in space. In fact, we are more interested in considering fingers which are kinematic mechanisms. For each finger i we associate a forward kinematic map $K_{f_i}: \mathbb{R}^{n_i} \to SE(3)$ which takes joint position to end effector position and orientation. The Jacobian of the forward kinematic map relates joint velocities to the end effector velocities,

$$\begin{pmatrix} v_{f_i} \\ \omega_{f_i} \end{pmatrix} = \frac{\partial K_{f_i}}{\partial \theta_{f_i}} \frac{d\theta}{dt} K_{f_i}^{-1} = J_{f_i}(\theta_{f_i})\dot{\theta}_{f_i}, \qquad \theta_{f_i} \in \mathbb{R}^{n_i},\ (v_{f_i}, \omega_{f_i}) \in \mathbb{R}^6 \tag{2.44}$$

Combining this with the velocity transformation between the finger location and the contact location (a function of $x_o^{-1}x_f$) we write the *contact Jacobian* as

$$J_{c_i}(x_o, \theta_{f_i}) = \begin{pmatrix} I & S(r_{c_i}) \\ 0 & I \end{pmatrix} J_{f_i} \qquad J_{c_i} : \dot{\theta} \mapsto \begin{pmatrix} v_{c_i} \\ \omega_{c_i} \end{pmatrix} \tag{2.45}$$

As with the fixed contacts, fingers are only allowed to exert forces in certain directions depending on the contact type. This is equivalent to saying that finger motions are only constrained in certain directions; these directions are given by the column span of $B_i^T(x_o, \theta_{f_i}): \mathbb{R}^{m_i} \to \mathbb{R}^6$ (where B_i is the selection matrix defined in Section 2.2). Combining this with the grasp map for the i^{th} finger, we obtain the velocity constraint due to the i^{th} contact,

$$G_i^T(x_o, \theta_{f_i}) \begin{pmatrix} v_o \\ \omega_o \end{pmatrix} = B_i^T(x_o, \theta_{f_i}) J_{c_i}(x_o, \theta_{f_i}) \dot{\theta}_{f_i} \tag{2.46}$$

We now stack these matrices and write the grasp constraint for the hand as

$$\begin{bmatrix} G_1^T \\ \vdots \\ G_k^T \end{bmatrix} \begin{pmatrix} v_o \\ \omega_o \end{pmatrix} = \begin{bmatrix} B_1^T J_{c_1} & & 0 \\ & \ddots & \\ 0 & & B_k^T J_{c_k} \end{bmatrix} \dot{\theta} \tag{2.47}$$

$$G^T(x_o, \theta) \begin{pmatrix} v_o \\ \omega_o \end{pmatrix} = J(x_o, \theta)\dot{\theta} \tag{2.48}$$

2.5 Grasp stability and manipulability

For contact models involving friction, we must insure that all contact forces lie within the friction cone determined by the coefficient of friction. The set of all forces lying in or on the friction cone is

$$FC = \left\{ f_c \in \mathbb{R}^n : \|f_{c_{ij}}^t\| \le \mu_{ij} \|f_{c_i}^n\|, \quad i = 1, \ldots, k, \quad j = 1, \ldots, m_i \right\} \tag{2.49}$$

where $f_{c_{ij}}^t$ is the tangent component of the j^{th} element of f_{c_i}, $f_{c_i}^n$ is the normal force for the i^{th} contact, and μ_{ij} is the coefficient of friction corresponding to $f_{c_{ij}}$. For soft finger contacts, the torques exerted by the fingers also satisfy equation (2.49) with $f^t_{c_{ij}}$ replaced by the torque (i.e., we do not want to apply a torque which is greater than the torsional friction coefficient multiplied by the magnitude of the normal force).

We say a grasp on an object is *stable* if we can resist, through a set of contacts, arbitrary forces and torques on the object. This requires that the image of the grasp map over the set of forces in the friction cone span the space of forces and torques on the object, that is $G(FC) = \mathbf{R}^6$. Note that this is a condition only on the contact kinematics and not the finger kinematics. A stable grasp is also called a *force closure* grasp.

A grasp is said to be *manipulable* if arbitrary motions of the object can be accommodated by the fingers. Unlike stability, manipulability is a property of both the contact and finger kinematics. Since the range of motion of the contacts is given locally by the range of the hand Jacobian, the condition can be written as $\mathcal{R}(G^T) \subseteq \mathcal{R}(J)$.

It is also useful to define the concept of prehensility. A grasp is *prehensile* if there exists a force contained in the null space of the grasp map which also lies in the *interior* of the friction cone. More formally, $\mathcal{N}(G) \cap \overset{\circ}{FC} \neq \{\}$ where $\overset{\circ}{FC}$ is the set of forces lying completely within the friction cone (i.e., $\|f^t_{c_{ij}}\| < \mu_{ij}\|f^n_{c_i}\|$). We shall require this property in order to insure that our controllers can maintain a grip on an object while manipulating it.

We shall generally assume that a grasp has been chosen which is stable, manipulable and prehensile. The problem of finding such grasps given a set of fingers and an object has been studied in some detail. A good treatment is given by Nguyen [14].

Appendix – Contact kinematics derivation

In this appendix we derive the kinematics of contact for two objects touching each other at a point. The notation is described more fully in Section 2.3. An alternate derivation can be found in a recent paper by Montana [12].

To derive the kinematics, we begin with constraint equations given by equating the points of contact, normals of contact and tangent planes at the contact points:

$$\begin{aligned} Rc_f(\alpha_f) + p &= c_o(\alpha_o) && (2.50)\\ Rn_f(\alpha_f) &= -n_o(\alpha_o) && (2.51)\\ R\frac{\partial c_f}{\partial \alpha_f} M_f^{-1} R_\psi &= \frac{\partial c_o}{\partial \alpha_o} M_o^{-1} && (2.52) \end{aligned}$$

Differentiate (2.50) and (2.51)

$$\begin{aligned} \dot{R}c_f + R\frac{\partial c_f}{\partial \alpha_f}\dot{\alpha}_f + \dot{p} &= \frac{\partial c_o}{\partial \alpha_o}\dot{\alpha}_o && (2.53)\\ \dot{R}n_f + R\frac{\partial n_f}{\partial \alpha_f}\dot{\alpha}_f &= -\frac{\partial n_o}{\partial \alpha_o}\dot{\alpha}_o && (2.54) \end{aligned}$$

Multiply (2.53) by $\frac{\partial c_o}{\partial \alpha_o}^T$ and substitute $\dot{\alpha}_o$ into (2.54)

$$\dot{R}n_f + R\frac{\partial n_f}{\partial \alpha_f}\dot{\alpha}_f = -\frac{\partial n_o}{\partial \alpha_o} M_o^{-2} \frac{\partial c_o}{\partial \alpha_o}^T \left(\dot{R}c_f + R\frac{\partial c_f}{\partial \alpha_f}\dot{\alpha}_f + \dot{p}\right) \qquad (2.55)$$

Using (2.52) in the last term of (2.55) and rearranging

$$\begin{aligned} &\left(R\frac{\partial n_f}{\partial \alpha_f} + \frac{\partial n_o}{\partial \alpha_o} M_o^{-2} (\frac{\partial c_o}{\partial \alpha_o}^T \frac{\partial c_o}{\partial \alpha_o}) M_o^{-1} R_\psi M_f\right)\dot{\alpha}_f \\ &= -\dot{R}n_f - \frac{\partial n_o}{\partial \alpha_o} M_o^{-2} \frac{\partial c_o}{\partial \alpha_o}^T (\dot{R}c_f + \dot{p}) \qquad (2.56) \end{aligned}$$

Simplify the first term and multiply by $M_o^{-T}\frac{\partial c_o}{\partial \alpha_o}^T$ on the left

$$\begin{aligned} &M_o^{-T}\frac{\partial c_o}{\partial \alpha_o}^T \left(R\frac{\partial n_f}{\partial \alpha_f} + \frac{\partial n_o}{\partial \alpha_o} M_o^{-1} R_\psi M_f\right) \\ &= M_o^{-T}\frac{\partial c_o}{\partial \alpha_o}^T \left(R\frac{\partial n_f}{\partial \alpha_f} M_f^{-1} R_\psi + \frac{\partial n_o}{\partial \alpha_o} M_o^{-1}\right) R_\psi M_f \\ &= \left(\underbrace{R_\psi M_f^{-T}\frac{\partial c_f}{\partial \alpha_f}^T \frac{\partial n_f}{\partial \alpha_f} M_f^{-1} R_\psi}_{\tilde{K}_f} + \underbrace{M_o^{-T}\frac{\partial c_o}{\partial \alpha_o}^T \frac{\partial n_o}{\partial \alpha_o} M_o^{-1}}_{K_o}\right) R_\psi M_f \qquad (2.57) \end{aligned}$$

Multiply both sides of (2.56) by $M_o^{-T}\frac{\partial c_o}{\partial \alpha_o}^T$ and use the previous calculation

$$\begin{aligned}
\dot{\alpha}_f &= M_f^{-1}R_\psi\left(\tilde{K}_f+K_o\right)^{-1}\cdot \\
&\qquad M_o^{-T}\frac{\partial c_o}{\partial \alpha_o}^T\left(-\dot{R}n_f-\frac{\partial n_o}{\partial \alpha_o}M_o^{-2}\frac{\partial c_o}{\partial \alpha_o}^T(\dot{R}c_f+\dot{p})\right) \\
&= M_f^{-1}R_\psi\left(\tilde{K}_f+K_o\right)^{-1}\cdot \\
&\qquad \left(-M_o^{-T}\frac{\partial c_o}{\partial \alpha_o}^T\dot{R}n_f-K_oM_o^{-T}\frac{\partial c_o}{\partial \alpha_o}^T(\dot{R}c_f+\dot{p})\right) \qquad (2.58)
\end{aligned}$$

Let ω_t stand for the $\dot{R}n_f$ term and v_t represent the $\dot{R}c_f+\dot{p}$ term:

$$\dot{\alpha}_f = M_f^{-1}R_\psi\left(\tilde{K}_f+K_o\right)^{-1}(w_t-K_ov_t) \qquad (2.59)$$

Now w_t and v_t can now be calculated in terms of the relative velocity given by $(\mathcal{S}(\omega),v)=\dot{g}g^{-1}$. We use the fact that $\mathcal{S}(\omega)a=\omega\times a$ and $\omega\times a=-a\times\omega$ to obtain

$$\begin{aligned}
w_t &= -M_o^{-T}\frac{\partial c_o}{\partial \alpha_o}^T(\omega\times(Rn_f)) = -M_o^{-T}\frac{\partial c_o}{\partial \alpha_o}^T(n_o\times\omega) \qquad (2.60) \\
v_t &= M_o^{-T}\frac{\partial c_o}{\partial \alpha_o}^T(\omega\times(Rc_f)+\omega\times p+v) \\
&= M_o^{-T}\frac{\partial c_o}{\partial \alpha_o}^T(\omega\times(c_o-p)+\omega\times p+v) \\
&= M_o^{-T}\frac{\partial c_o}{\partial \alpha_o}^T(-c_o\times\omega+v) \qquad (2.61)
\end{aligned}$$

We see that ω_t is the relative rotational velocity projected onto the tangent plane at the contact. It includes only terms due to *rolling* since rotation normal to the surface is annihilated by taking the cross product with n_o. Likewise, v_t is the relative linear velocity between the contacts, projected onto the tangent plane, i.e., the *sliding* velocity.

A similar calculation yields

$$\dot{\alpha}_o = M_o^{-1}\left(\tilde{K}_f+K_o\right)^{-1}\left(w_t-\tilde{K}_fv_t\right) \qquad (2.62)$$

which gives the kinematics for the object contact point in local coordinates.

Next we solve for ψ, the angle between the tangent planes of the finger and object. Combining (2.51) and (2.52) we can write

$$R\begin{bmatrix} \frac{\partial c_f}{\partial \alpha_f}M_f^{-1} & n_f \end{bmatrix}\begin{bmatrix} R_\psi & 0 \\ 0 & -1 \end{bmatrix} = \begin{bmatrix} \frac{\partial c_o}{\partial \alpha_o}M_o^{-1} & n_o \end{bmatrix} \qquad (2.63)$$

and using the normalized gaussian coordinates this can be rewritten

$$R[x_f\ y_f\ z_f]\bar{R}_\psi = [x_o\ y_o\ z_o] \tag{2.64}$$

Take the derivative of (2.64)

$$\dot{R}[x_f\,y_f\,z_f]\bar{R}_\psi + R[\dot{x}_f\,\dot{y}_f\,\dot{z}_f]\bar{R}_\psi + R[x_f\,y_f\,z_f]\begin{bmatrix} \dot{R}_\psi & 0 \\ 0 & 0 \end{bmatrix} = [\dot{x}_o\,\dot{y}_o\,\dot{z}_o] \tag{2.65}$$

Premultiply by $y_f^T R^T$

$$y_f^T R^T \dot{R}[x_f\,y_f\,z_f]\bar{R}_\psi + y_f^T[\dot{x}_f\,\dot{y}_f\,\dot{z}_f]\bar{R}_\psi + (0\,1\,0)\begin{bmatrix} \dot{R}_\psi 0 \\ 0\ 0 \end{bmatrix} = y_f^T R^T[\dot{x}_o\,\dot{y}_o\,\dot{z}_o] \tag{2.66}$$

Postmultiply by $\bar{R}_\psi \begin{pmatrix} 1 \\ 0 \\ 0 \end{pmatrix}$ and note $\bar{R}_\psi \bar{R}_\psi = I$

$$y_f^T R^T \dot{R} x_f + y_f^T \dot{x}_f + (0\,1\,0)\begin{bmatrix} \dot{R}_\psi R_\psi & 0 \\ 0 & 0 \end{bmatrix}\begin{pmatrix} 1 \\ 0 \\ 0 \end{pmatrix} = y_f^T R^T[\dot{x}_o\,\dot{y}_o\,\dot{z}_o]\bar{R}_\psi \begin{pmatrix} 1 \\ 0 \\ 0 \end{pmatrix} \tag{2.67}$$

$$y_f^T R^T \dot{R} x_f + y_f^T \dot{x}_f + (0\,1)\begin{bmatrix} 0 & \dot{\psi} \\ -\dot{\psi} & 0 \end{bmatrix}\begin{pmatrix} 1 \\ 0 \end{pmatrix} = y_f^T R^T[\dot{x}_o\,\dot{y}_o\,\dot{z}_o]\bar{R}_\psi \begin{pmatrix} 1 \\ 0 \\ 0 \end{pmatrix} \tag{2.68}$$

$$y_f^T R^T \dot{R} x_f + y_f^T \dot{x}_f - \dot{\psi} = y_f^T R^T[\dot{x}_o\,\dot{y}_o\,\dot{z}_o]\bar{R}_\psi \begin{pmatrix} 1 \\ 0 \\ 0 \end{pmatrix} \tag{2.69}$$

From (2.64) we see that $y_f^T R^T = (0\,1\,0)\bar{R}_\psi \begin{bmatrix} x_o^T \\ y_o^T \\ z_o^T \end{bmatrix} = (0\,1)R_\psi \begin{bmatrix} x_o^T \\ y_o^T \end{bmatrix}$ and so

$$\dot{\psi} = y_f^T R^T \dot{R} x_f + y_f^T \frac{\partial x_f}{\partial \alpha_f}\dot{\alpha}_f - (0\,1)R_\psi \begin{bmatrix} x_o^T \dot{x}_o & x_o^T \dot{y}_o \\ y_o^T \dot{x}_o & y_o^T \dot{y}_o \end{bmatrix} R_\psi \begin{pmatrix} 1 \\ 0 \end{pmatrix} \tag{2.70}$$

Using the following identities

$$\begin{aligned} x_i^T y_i = 0 \quad &\Rightarrow \quad \dot{x}_i^T y_i = -x_i^T \dot{y}_i = y_i^T \dot{x}_i \\ x_i^T x_i = 1 \quad &\Rightarrow \quad \dot{x}_i^T x_i = 0 \end{aligned} \tag{2.71}$$

(2.70) can be written as

$$\begin{aligned} \dot{\psi} &= y_f^T R^T \dot{R} x_f + y_o^T \frac{\partial x_o}{\partial \alpha_o}\dot{\alpha}_o + y_f^T \frac{\partial x_f}{\partial \alpha_f}\dot{\alpha}_f \\ &= \omega_n + T_o M_o \dot{\alpha}_o + T_f M_f \dot{\alpha}_f \end{aligned} \tag{2.72}$$

where

$$\begin{aligned} \omega_n &= y_f^T R^T \dot{R} x_f = (R y_f)^T \omega \times (R x_f) \\ &= (R z_f)^T \omega = z_o^T \omega \end{aligned} \tag{2.73}$$

and the last equality follows from the vector formula $a \cdot b \times c = b \cdot c \times a$. This last equation shows that ω_n is just the relative rotational velocity projected onto the surface normal.

Collecting equations (2.59), (2.62) and (2.72) we have

$$\begin{aligned}
\dot{\alpha}_o &= M_o^{-1}(K_o + \tilde{K}_f)^{-1}\left(\omega_t - \tilde{K}_f v_t\right) &(2.74)\\
\dot{\alpha}_f &= M_f^{-1} R_\psi (K_o + \tilde{K}_f)^{-1}(\omega_t - K_o v_t) &(2.75)\\
\dot{\psi} &= \omega_n + T_o M_o \dot{\alpha}_o + T_f M_f \dot{\alpha}_f &(2.76)
\end{aligned}$$

The matrix $K_o + \tilde{K}_f$ is called the *relative curvature* by Montana[12].

Chapter 3

Dynamics and Control

In this section we review some basic results in dynamics of robot systems. The primary result which we present is that even for relatively complicated robot systems, the equations of motion for the system can be written in a standard form. This point of view has been used by Khatib in his operational space formulation [6] and in some recent extensions [7]. The results presented in this section are direct extensions of those works, although the approach is different.

3.1 Robot dynamics

We begin by deriving the robot dynamics for a manipulator in joint space. Let $\theta \in \mathbb{R}^n$ be the joint angles for the manipulator and $\tau \in \mathbb{R}^n$ be the corresponding joint torques. The Lagrangian for the system may be shown to be of the form

$$L = M(\theta)(\dot{\theta}, \dot{\theta}) + V(\theta) \tag{3.1}$$

where $M(\theta)$ is the inertia matrix for the manipulator and $V(\theta)$ is the potential energy due to gravity. Substituting into Lagrange's equations

$$\left(\frac{d}{dt} \frac{\partial L}{\partial \dot{\theta}} - \frac{\partial L}{\partial \theta} - \tau \right) \delta\theta = 0 \tag{3.2}$$

and letting τ represent the actuator torques (and other non-conservative forces), we obtain

$$M(\theta)(\ddot{\theta}, \cdot) + DM(\theta)(\dot{\theta}, \cdot)(\dot{\theta}) - \frac{1}{2} DM(\theta)(\dot{\theta}, \dot{\theta})(\cdot) + DV(\theta)(\cdot) = \tau \tag{3.3}$$

To put this in a more conventional form we define the matrix $C(\theta, \dot{\theta})$ as

$$a^T C(\theta, \dot{\theta}) b = \frac{1}{2} DM(\theta)(\dot{\theta}, a)(b) + \frac{1}{2} DM(\theta)(b, a)(\dot{\theta}) - \frac{1}{2} DM(\theta)(\dot{\theta}, b)(a) \tag{3.4}$$

and write

$$M(\theta)\ddot{\theta} + C(\theta, \dot{\theta})\dot{\theta} + N(\theta, \dot{\theta}) = \tau \tag{3.5}$$

where $N(\theta, \dot{\theta})$ includes gravity terms and other forces (such as friction) which act at the joints.

For systems of this type, the inertia matrix is always symmetric and positive definite and it can be shown that $\dot{M} - 2C$ is skew symmetric (using this particular choice of C). It is both the form and the structure of this equation that we will attempt to maintain in more complicated systems.

3.2 Robot hand dynamics

We now examine the dynamics of a set of fingers actuated at each joint connected through a set of contacts to a rigid body. The finger dynamics can be written as

$$M_f(\theta)\ddot{\theta} + C_f(\theta, \dot{\theta})\dot{\theta} + N_f(\theta, \dot{\theta}) = \tau \tag{3.6}$$

where $\theta \in \mathbf{R}^{n_1} \times \cdots \times \mathbf{R}^{n_k}$ is now the set of joint angles for *all* of the robots and τ is the corresponding set of torques. The object dynamics are given by the Newton-Euler equations

$$\begin{bmatrix} m_o I & 0 \\ 0 & \mathcal{I}_o \end{bmatrix} \begin{pmatrix} \dot{v}_o \\ \dot{\omega}_o \end{pmatrix} + \begin{pmatrix} 0 \\ \omega_o \times \mathcal{I}_o \omega_o \end{pmatrix} + \begin{pmatrix} DV_o(x_o) \\ 0 \end{pmatrix} = \begin{pmatrix} f_o \\ \tau_o \end{pmatrix} \tag{3.7}$$

where $\mathcal{I}_o = R\mathcal{I}R^T$ is the object inertia in world coordinates and V_o is the potential energy. In local coordinates this has the same basic form as the robot dynamics, lacking only the actuator torques:

$$M_o(x)\ddot{x} + C_o(x, \dot{x})\dot{x} + N_o(x, \dot{x}) = 0 \tag{3.8}$$

where x is a local parameterization of $x_o \in SE(3)$. We attach these two systems with a set of constraints

$$G^T(x, \theta)\dot{x} = J(x, \theta)\dot{\theta} \tag{3.9}$$

which represents the grasp. We will assume that the grasp is both stable and manipulable. For the moment we will also require J to be injective.

This velocity constraint generates a constraint on the virtual displacements $\delta\theta$ and δx, namely $\delta\theta = J^{-1}(q)G^T(q)\delta x$ with $q = (x, \theta)$. Using this relationship, we can write Lagrange's equations as

$$\left(\frac{d}{dt}\frac{\partial L}{\partial q} - \frac{\partial L}{\partial q} - (\tau, 0)\right)\delta q = 0 \tag{3.10}$$

$$\begin{pmatrix} \frac{d}{dt}\frac{\partial L}{\partial \dot{\theta}} - \frac{\partial L}{\partial \theta} - \tau \\ \frac{d}{dt}\frac{\partial L}{\partial \dot{x}} - \frac{\partial L}{\partial x} \end{pmatrix} \begin{pmatrix} \delta\theta \\ \delta x \end{pmatrix} = 0 \tag{3.11}$$

$$\left(\frac{d}{dt}\frac{\partial L}{\partial \dot{\theta}} - \frac{\partial L}{\partial \theta} - \tau\right)\delta\theta + \left(\frac{d}{dt}\frac{\partial L}{\partial \dot{x}} - \frac{\partial L}{\partial x}\right)\delta x = 0 \quad (3.12)$$

$$GJ^{-T}\left(\frac{d}{dt}\frac{\partial L}{\partial \dot{\theta}} - \frac{\partial L}{\partial \theta} - \tau\right)\delta x + \left(\frac{d}{dt}\frac{\partial L}{\partial \dot{x}} - \frac{\partial L}{\partial x}\right)\delta x = 0 \quad (3.13)$$

and since δx is arbitrary

$$\frac{d}{dt}\frac{\partial L}{\partial \dot{x}} - \frac{\partial L}{\partial x} + GJ^{-T}\left(\frac{d}{dt}\frac{\partial L}{\partial \dot{\theta}} - \frac{\partial L}{\partial \theta}\right) = GJ^{-T}\tau \quad (3.14)$$

This equation together with the velocity constraint given in equation (3.9) describes the system completely. Note that equation (3.14) is a vector differential equation with $n - m$ rows and equation (3.9) is a vector equation with m rows.

It is tempting to derive equation (3.14) by using the velocity constraint directly in the kinetic energy equation (which is a function of $\dot{\theta}$ and $\dot{x}$) and then substituting this into Lagrange's equations. As noted in Rosenberg [15] this can only be done if the constraint is holonomic, i.e., θ can be written as a function of x.

Next we separate the kinetic energy into an object portion and a robot portion

$$T = \dot{\theta}^T M_f(\theta)\dot{\theta} + \dot{x}^T M_o(x)\dot{x} \quad (3.15)$$

Using equation (3.14) we find

$$\tilde{M}(q)\ddot{x} + \tilde{C}(q, \dot{q})\dot{x} = GJ^{-T}\tau = F \quad (3.16)$$

where

$$\begin{aligned} \tilde{M} &= M_o + GJ^{-T}M_f J^{-1}G^T \\ \tilde{C} &= C_o + GJ^{-T}\left(C_f J^{-1}G^T + M_f \frac{d}{dt}\left(J^{-1}G^T\right)\right) \end{aligned}$$

and C_f and C_o are obtained from equation (3.4) by replacing M with M_f and M_o respectively. It can be shown that the matrix $\dot{\tilde{M}} - 2\tilde{C}$ is still skew symmetric.

Thus we have an equation with form (and structure) similar to our "simple" robot. In the object frame of reference, $\tilde{M}$ is the effective mass of the object, and $\tilde{C}$ is the effective Coriolis and centrifugal matrix. These matrices include the dynamics of the fingers, which are being used to actually control the motion of the object. However the details of the finger kinematics and dynamics are effectively hidden in the definition of $\tilde{M}$ and $\tilde{C}$.

This simple result has some interesting consequences in control. Typically robot controllers are designed by placing a feedback loop around the joint positions (and velocities) of the robot. The controller generates torques which attempt to make the robot follow a prescribed joint trajectory. This can lead to difficulty in grasping situations since the joint level controllers are often not aware of the constraints and therefore may violate them. However, since the grasping dynamics are of the same form as the dynamics of a single manipulator, we can just as easily write the control algorithm in object coordinates. An additional advantage of this approach is that controller objectives are often specified in terms of the object motion and hence it might be easier to perform the controller design and analysis in that space.

Even though we will write our controllers in terms of F, it is actually the joint torques which we are able to specify. Given the desired force in constrained coordinates, we can apply that force using an actuator force of $J^T G^+ \tau$, where G^+ is a pseudo-inverse for G. In general G is not square and by examining the right side of the equations of motion (3.16) we note that if $J^{-T}\tau \in \mathcal{N}(G)$ then the net force in the object frame of reference is zero and hence forces of this form cause no net motion on the object. These forces are in fact the forces which act against the constraint and are generally termed *internal* or *constraint* forces. We can use these internal forces to satisfy other conditions, such as keeping the contact forces inside the friction cone (to avoid slipping) or varying the load distribution of a set of manipulators rigidly grasping an object.

Redundant manipulators

Some manipulators contain more degrees of freedom than are necessary to specify the position of the end effector. Mathematically, these robots can be represented by a change of coordinates $f\colon \mathbb{R}^m \to \mathbb{R}^n$ where $m > n$. In this case $J := \frac{\partial f}{\partial \theta}$ is not square and hence J^{-1} is not well defined so our derivation of equation (3.16) does not hold.

It is still possible to write the dynamics of redundant manipulators in a form consistent with equation (3.16). To do so, we first define a matrix $K(\theta)$ whose rows span the null space of $J(\theta)$. As before we assume that $J(\theta)$ is full row rank and hence $K(\theta)$ has constant rank $m-n$. The rows of $K(\theta)$ are basis elements for the space of velocities which cause no motion of the end effector; we can thus define an *internal motion*, $\dot{y} \in \mathbb{R}^{m-n}$ using the equation

$$\begin{pmatrix} \dot{x} \\ \dot{y} \end{pmatrix} = \begin{bmatrix} J \\ K \end{bmatrix} \dot{\theta} \tag{3.17}$$

and our constraint becomes

$$\bar{J}\dot{\theta} = \begin{bmatrix} J \\ K \end{bmatrix} \dot{\theta} = \begin{bmatrix} G^T & 0 \\ 0 & I \end{bmatrix} \begin{bmatrix} \dot{x} \\ \dot{y} \end{bmatrix} = \bar{G}\begin{pmatrix} \dot{x} \\ \dot{y} \end{pmatrix} \tag{3.18}$$

The kinetic energy can be written

$$T = \dot{\theta}^T M_f(\theta)\dot{\theta} + \begin{pmatrix} \dot{x} \\ \dot{y} \end{pmatrix}^T \begin{bmatrix} M_o & 0 \\ 0 & 0 \end{bmatrix} \begin{pmatrix} \dot{x} \\ \dot{y} \end{pmatrix} \tag{3.19}$$

and since $\bar{J}$ is invertible it follows from our previous derivation that

$$\tilde{M}(q)\begin{pmatrix}\ddot{x}\\ \ddot{y}\end{pmatrix}+\tilde{C}(q,\dot{q})\begin{pmatrix}\dot{x}\\ \dot{y}\end{pmatrix}+\tilde{N}(q,\dot{q})=\bar{G}\bar{J}^{-T}\tau \tag{3.20}$$

where $\tilde{M}$ and $\tilde{C}$ are obtained as in the nonredundant case but replacing J with $\bar{J}$ and G with $\bar{G}$. If we choose K such that its rows are orthonormal then $\bar{J}^{-1} = (J^+ \; K^T)$ where $J^+ = J^T(JJ^T)^{-1}$ is the least-squares right (pseudo) inverse of J.

As before, the structure of the robot dynamics is maintained. However, the inertia and Coriolis/centrifugal matrices are functions of the robot configuration, θ, and not the end effector configuration, x. This complication is unavoidable due to the non-uniqueness of the inverse kinematic problem. In principle, one could locally parameterize the redundant motion by y (the integral of $\dot{y}$), allowing these matrices to be written as functions of both x and y; we will not assume that such a parameterization is available.

3.3 Control

The grasping control problem can be broken into two parts

1. Tracking – the center of mass of the object should follow a specified trajectory.
2. Holding – the finger forces should lie within the friction cone at all times.

Condition 2 is important not only because we do not wish to lose our grip on the object, but also because we assumed in our derivation of the grasp dynamics that contact was maintained. Without this constraint we would have to specify the dynamics of contact.

If a grasp is prehensile it can be shown that given an arbitrary set of finger forces, F_c, we can find an internal force, $F_N \in \mathcal{N}(G)$, such that the combined force $F_c + F_N$ is inside the friction cone. Thus, given a force generated to solve the tracking problem, we can always add a force to this such that condition 2 is satisfied. Since internal forces cause no net motion of the hand or object, this additional force does not affect the net force exerted by the fingers on the object. We shall assume in the sequel that such an internal force is available at all times. The choice of this force is discussed in more detail below.

To illustrate the control of robot systems, we look at two controllers which have appeared in the robotics literature. We consider only grasps which are stable, manipulable and prehensile. We start by considering systems of the form

$$M(q)\ddot{x}+C(q,\dot{q})\dot{x}+N(q,\dot{q})=F \tag{3.21}$$

where $M(q)$ is a positive definite inertia matrix and $C(q,\dot{q})\dot{x}$ is the Coriolis and centrifugal force vector. The vector $N(q,\dot{q}) \in \mathbb{R}^n$ contains all friction and gravity terms and the vector $F \in \mathbb{R}^n$ represents generalized forces in the object coordinate frame. Given an object force F, we apply that force by commanding a set of joint torques

$$\tau = J^T G^+ F + J^T F_N \tag{3.22}$$

where J and G define the grasping constraint and $F_N \in \mathcal{N}(G)$.

Computed torque

Computed torque is an exactly linearizing control law (i.e., the dynamics are rendered linear by state feedback) that has been used extensively in robotics research. It has been used for joint level control [1], Cartesian control [11], and most recently, control of multi-fingered hands [10, 4]. Given a desired trajectory x_d we use the control

$$F = M(q)\left(\ddot{x}_d + K_v \dot{e} + K_p e\right) + C(q, \dot{q})\dot{x} + N(q, \dot{q}) \tag{3.23}$$

where error $e = x_d - x$ and K_v and K_p are constant gain matrices. The resulting dynamics equations are linear with exponential rate of convergence determined by K_v and K_p. Since the system is linear, we can use linear control theory to choose the gains (K_v and K_p) such that they satisfy some set of design criteria.

The disadvantage of this control law is that it is not easy to specify the interaction with the environment. From the form of the error equation we might think that we could use K_p to model the stiffness of the system and exert forces by commanding trajectories which result in fixed errors. Unfortunately this is not uniformly applicable as can be seen by examining the force due to a quasi-static displacement Δx:

$$\Delta F = M(q) K_p \Delta x \tag{3.24}$$

Since K_p must be constant in order to prove stability, the resultant stiffness will vary with configuration. Additionally, given a desired stiffness matrix it may not be possible to find a positive definite K_p that achieves that stiffness.

'PD' control

PD controllers differ from computed torque controllers in that the desired stiffness (and potentially damping) of the end effector is specified, rather than its position tracking characteristics. Typically, control laws of this form rely on the skew symmetric property of robot dynamics, namely $\alpha^T \left(\dot{M} - 2C\right) \alpha = 0$ for all $\alpha \in \mathbb{R}^n$, for proof of stability. Consider the control law

$$F = M(q)\ddot{x}_d + C(q, \dot{q})\dot{x}_d + N(q, \dot{q}) + K_v \dot{e} + K_p e \tag{3.25}$$

where K_v and K_p are symmetric positive definite. Using a Liapunov stability argument, it can be shown that the actual trajectory of the robot converges to the desired trajectory asymptotically [8]. Extensions to the control law result in exponential rate of convergence [17, 16].

This PD control law has the advantage that for a quasi-static change in position Δx the resulting force is

$$\Delta F = K_p \Delta x \tag{3.26}$$

and thus we can achieve an arbitrary symmetric stiffness. Experimental results indicate that the trajectory tracking performance of this control law does not always compare favorably with the computed torque control law [13]. Additionally there is no simple design criteria for choosing K_v and K_p to achieve good tracking performance. While the stability results give necessary conditions for stability they do not provide a method for choosing the gains. Nonetheless, PD control has been used effectively in many robot controllers and has some computational features which make it an attractive alternative.

Internal forces

All of the controllers rely on the choice of a grasping force, $F_N \in \mathcal{N}(G)$ which maintains contact between the fingertips and the object by insuring that the finger forces lie in the friction cone. There are several possible methods for calculating this term. Since F_N does not affect the motion of the object, its choice does not affect object tracking. We begin by showing that given any desired object force, there exists a set of finger forces lying in the friction cone which achieves it.

Proposition 2 *If a grasp is prehensile, given any $F_c \in \mathbb{R}^m$, there exists a null force, F_N, such that the total finger force, $F_c + F_N$, is inside the friction cone.*

Proof. By the definition of a prehensile grasp there exists $F_N \in \mathcal{N}(G) \cap \overset{\circ}{FC}$ such that

$$||F^t_{N_{ij}}|| < \mu_i ||F^n_{N_i}|| \tag{3.27}$$

where $F^t_{N_{ij}}$ is the tangent component of F_N projected onto the j^{th} force direction of the i^{th} contact and F_{N_i} is the normal component of F_N at the i^{th} contact point F_{N_i} is nonzero for each i and therefore by increasing F_N, we always increase the normal component of the force exerted at each contact with respect to the tangential forces. Since $\overset{\circ}{FC}$ is defined as the Cartesian product of the n friction cones in equation (3.27), $F_N \in \mathcal{N}(G) \cap \overset{\circ}{FC}$ implies $\alpha F_N \in \mathcal{N}(G) \cap \overset{\circ}{FC}$ for all $\alpha \in \mathbb{R}^+$. Now we can look at the unit vector in the $F_c + \alpha F_N$ direction as $\alpha \to \infty$:

$$\lim_{\alpha \to \infty} \frac{F_c + \alpha F_N}{||F_c + \alpha F_N||} = F_N \tag{3.28}$$

Since $F_N \in \overset{\circ}{FC}$ it follows that for sufficiently high α, $\frac{F_c+\alpha F_N}{\|F_c+\alpha F_N\|}$ is also in $\overset{\circ}{FC}$ and hence $F_c + \alpha F_N$ is in the interior of the FC. Now from the definition of FC, the individual contact forces must all lie within their respective friction cones simultaneously. □

The simplest F_N is a constant F_N. It must be large enough so that finger forces never leave the friction cone over the entire trajectory of the object. Generally this requires a knowledge of the bounds on the external forces that can be exerted on the object. The advantage of this approach is that $J_h^T F_N$ can be calculated at the same rate as J_h—saving computation time.

A more robust F_N could be calculated by looking at the finger forces—these can be derived from the joint torques, τ, using $F_c = J_h^{-T}\tau$—and finding a null force which causes $F_c + F_N$ to lie in FC. If the grasp map has a simple form, such as the one given in the example in Section 2.2, a basis for the null space can be used to construct the set of all valid F_N. This calculation takes time but may be necessary in the case of large uncertainties.

Other grasp force calculations are discussed in [10] but all of these share some fundamental problems. One difficulty is that in a real-world hand the maximum motor torques that can be generated are finite. Thus, we are not guaranteed that we can apply an F_N which satisfies $F_c + F_N \in FC$ without saturating the motors. Another issue is the effect of the null force term in the presence of errors. If a large internal force term is used and, due to sensor or actuator errors, it does not actually lie in the null space of the grasp matrix, the resulting force can cause positioning errors and in the extreme case, instability.

Redundant motion

In addition to internal forces, fingers with excess degrees of freedom can have internal motions which do not cause motion of the fingers. Controllers must be extended to take into account this redundant motion. This is fundamentally no different than control of an ordinary finger except that position information is not available in redundant directions. Thus the computed torque law would become

$$F = M(q)\begin{pmatrix} \ddot{x}_d + K_v\dot{e}_x + K_p e_x \\ \ddot{y}_d + K_v\dot{e}_y \end{pmatrix} + C(q,\dot{q})\begin{pmatrix} \dot{x} \\ \dot{y} \end{pmatrix} + N(q,\dot{q}) \tag{3.29}$$

Motion specification for such a control law would be in terms of a position trajectory $x_d(\cdot)$ and a velocity trajectory $\dot{y}_d(\cdot)$.

Chapter 4

Planning

Chapter 3 was dedicated to establishing control laws under which a grasped object moved along a specified trajectory denoted $x_d(t)$. This is useful in the instance that the task involved does not necessitate a change of grasp. This is not to say that the model and control laws do not allow for fingers to roll on the surface of the object. Indeed, in this instance the motion of the finger tips described by the equations (2.31) will determine where the grasp points go and how the grasp map changes during the course of the manipulation. However, there is no explicit control of the locations of the fingertips on the surface of the object. There are however a number of applications in which an object needs to be moved while the fingers are being repositioned in some controlled fashion on the surface of the object: for instance, twirling a baton or regrasping an object for greater stability or manipulability. In this chapter we will discuss the planning of individual finger motions on the surface of an object.

4.1 Dynamic finger repositioning

In Chapter 2, we derived the kinematic equations of contact for a single finger rolling on a body. We will aggregate these into a composite equation for all of the fingers. To review the notation of Chapter 2, we recall that $g_i = x_o x_{f_i}^{-1}$ stands for the position and orientation of the i^{th} finger ($x_{f_i} \in SE(3)$) relative to the body ($x_o \in SE(3)$). Also $\eta_i = (\alpha_{o_i}, \alpha_{f_i}, \psi_i)$ is the vector of the i^{th} contact coordinates with $\alpha_{o_i} \in \mathbb{R}^2$ standing for the surface representation of the object, $\alpha_{f_i} \in \mathbb{R}^2$ the surface representation of the i^{th} finger and ψ_i, the angle of contact (angle between the two orthogonal surface frames). The equations (2.31) can then be written as

$$\dot{\eta}_i = B_i(x_o, \eta_i) \begin{pmatrix} v_t \\ \omega_t \end{pmatrix} \tag{4.1}$$

where $B_i(x_o, \eta_i)$ represents the contact kinematics,

$$\begin{pmatrix} v_t \\ \omega_t \end{pmatrix} = \begin{bmatrix} M_o^{-T} \frac{\partial c_o}{\partial \alpha_o}^T & 0 \\ 0 & M_o^{-T} \frac{\partial c_o}{\partial \alpha_o}^T \end{bmatrix} \begin{bmatrix} I & S(n_o) \\ 0 & S(c_o) \end{bmatrix} \begin{pmatrix} v_i \\ \omega_i \end{pmatrix} \tag{4.2}$$

and

$$\begin{pmatrix} v_i \\ \omega_i \end{pmatrix} = \dot{g}_i g_i^{-1} \tag{4.3}$$

In turn, v and ω are linear functions of $v_o, \omega_o, v_{f_i}, \omega_{f_i}$ so that (4.1) may be rewritten as

$$\dot{\eta}_i = \bar{B}_i(x_o, \eta_i) \begin{pmatrix} v_o \\ \omega_o \\ v_{f_i} \\ \omega_{f_i} \end{pmatrix} \tag{4.4}$$

Aggregating equations (4.4) for $i = 1, \ldots, k$ and using the Jacobian of the finger kinematics (2.44) we have

$$\dot{\eta} = \bar{B}(x_o, \eta) \begin{pmatrix} v_o \\ \omega_o \\ \dot{\theta} \end{pmatrix} \tag{4.5}$$

where

$$\bar{B}(x_o, \eta) = \bar{B}(x_o, \eta) \begin{bmatrix} I & 0 \\ 0 & J_f(\theta) \end{bmatrix} \tag{4.6}$$

Also, the grasping constraint (cf. equation (2.48)) is given by

$$G^T(x_o, \theta) \begin{pmatrix} v_o \\ \omega_o \end{pmatrix} = J(x_o, \theta)\dot{\theta} \tag{4.7}$$

If the grasp map G is onto (the grasp map is stable) we can uniquely solve for (v_o, ω_o) in (4.7) as

$$\begin{pmatrix} v_o \\ \omega_o \end{pmatrix} = G^+(x_o, \theta) J(x_o, \theta)\dot{\theta} \tag{4.8}$$

Using (4.8) in (4.5) we have

$$\dot{\eta} = \bar{B}(x_o, \eta) \begin{bmatrix} G^+(x_o, \theta) J(x_o, \theta) \\ I \end{bmatrix} \dot{\theta} \tag{4.9}$$

We have determined that η is a smooth bijection of $x_o^{-1} x_f$. Further provided that the fingers do not have more than 6 degrees of freedom, x_f (locally) uniquely determines θ. Consequently (4.9) can be rewritten as

$$\dot{\eta} = \hat{B}(x_o, \eta)\dot{\theta} \tag{4.10}$$

Noting that the left hand side of (4.8) determines x_o, we now combine (4.8) and (4.10) as follows: define

$$\dot{\theta} = \dot{\theta}_1 + \dot{\theta}_2 \tag{4.11}$$

where $\dot{\theta}_1 \in \mathcal{R}(J^T(x_o, \theta))$ and $\dot{\theta}_2 \in \mathcal{N}(J(x_o, \theta))$. Further, define

$$u_1 = G^+(x_o, \theta) J(x_o, \theta) \dot{\theta}_1 x_o \tag{4.12}$$

Note that the map between u_1 and $\dot{\theta}_1$ is a bijection and let

$$\dot{\theta}_2 = K(x_o, \theta) u_2 \tag{4.13}$$

where the columns of $K(x_o, \theta)$ span the null space of $J(x_o, \theta)$. Using these two definitions it may be seen that (4.8) and (4.9) can be written as

$$\begin{aligned} \dot{x}_o &= u_1 \\ \dot{\eta} &= B_1(x_o, \eta) u_1 + B_2(x_o, \eta) u_2 \end{aligned} \tag{4.14}$$

Thus the problem of finger repositioning and body manipulation can be reformulated as the problem of steering the states (x_o, η) of the control system (4.14). In the previous chapter we neglected the u_2 and considered the problem of steering x_o (u_1 was referred to as $\dot{x}_d$). There are as many u_2 as the dimension of the null space of $J(x_o, \theta)$. Away from kinematic singularities this dimension is

$$\sum_{i=1}^{k} \max\,(n_i - m_i, 0) \tag{4.15}$$

Recall that n_i is the number of joints in the i^{th} finger and m_i is determined by the contact type of the i^{th} finger. The formula above represents the number of extra finger degrees of freedom available to reposition the fingers. Note also that even if $u_2 = 0$ (i.e. no extra finger degrees of freedom) it may still be possible to steer both x_o, η using the u_1 alone.

With this discussion by way of preamble, we begin a detailed of steering systems of the form

$$\dot{x} = B(x) u \tag{4.16}$$

with $x \in \mathbb{R}^n, u \in \mathbb{R}^m$. Note that our steering problem really is a steering problem on a nontrivial manifold $SE(3) \times \mathbb{R}^{5k}$ ((x_o, η) space) rather than $\mathbb{R}^n$ but we will content ourselves with a local discussion, namely on a coordinate chart of $SE(3) \times \mathbb{R}^{5k}$.

4.2 Review of Optimal Control

Following Brockett [2], we will review some results from optimal control. Consider control systems of the form

$$\dot{x} = B(x) u \tag{4.17}$$

Here $x \in \mathbf{R}^n$, $u \in \mathbf{R}^m$ and $B(x) \in \mathbf{R}^{n\times m}$. The optimal control problem is to minimize

$$\frac{1}{2}\int_0^1 |u|^2 dt \tag{4.18}$$

subject to the conditions $x(0) = x^i$, $x(1) = x^f$. When $m < n$, this problem is a geodesic problem with a singular Riemannian metric specified by the equations (4.17) and (4.18). From Chow's theorem, it follows that this problem has a solution for arbitrary x^i, x^f if and only if the involutive closure of the vector fields described by the columns of $B(x)$ is all of $\mathbf{R}^n$.

It is instructive to analyze some sample solutions to this problem which are in some sense canonic. We start with $n = 3$ and $m = 2$:

$$\begin{aligned} \dot{x}_1 &= u_1 \\ \dot{x}_2 &= u_2 \\ \dot{x}_3 &= x_1 u_2 - x_2 u_1 \end{aligned} \tag{4.19}$$

with $x(0) = (0,0,0)$ and $x(1) = (0,0,a)$. The cost function may be written as

$$\min \frac{1}{2}\int_0^1 (\dot{x}_1^2 + \dot{x}_2^2) dt \tag{4.20}$$

with the control system (4.19) written as a constraint

$$\dot{x}_3 = x_2 \dot{x}_1 - x_1 \dot{x}_2 \tag{4.21}$$

From standard calculus of variations we may write the Euler-Lagrange equations with $\lambda(t)$ denoting the Lagrange multiplier as

$$\begin{aligned} \ddot{x}_1 - \lambda \dot{x}_2 &= 0 \\ \ddot{x}_2 + \lambda \dot{x}_1 &= 0 \\ \dot{\lambda} &= 0 \end{aligned} \tag{4.22}$$

Equation (4.22) establishes that $\lambda(t)$ is constant and using equation (4.19) we see that

$$\begin{bmatrix} \dot{u}_1 \\ \dot{u}_2 \end{bmatrix} = \begin{bmatrix} 0 & \lambda \\ -\lambda & 0 \end{bmatrix} \begin{bmatrix} u_1 \\ u_2 \end{bmatrix} = \Lambda \begin{bmatrix} u_1 \\ u_2 \end{bmatrix} \tag{4.23}$$

so that

$$\begin{pmatrix} u_1(t) \\ u_2(t) \end{pmatrix} = e^{\Lambda t} u(0) \tag{4.24}$$

Consequently, since $x_1(0) = x_2(0) = 0$

$$\begin{pmatrix} x_1(t) \\ x_2(t) \end{pmatrix} = (e^{\Lambda t} - I)\, b; \qquad b = \Lambda^{-1} u(0) \tag{4.25}$$

Further, because $x_1(1) = x_2(1) = 0$, we have that $\lambda = 2n\pi$ so as to make $e^{\Lambda} = I$. Using this fact and noticing $\dot{x}_3 = \lambda/2\,(x_1^2 + x_2^2)$ it follows that

$$x_3(1) = x_3(0) + \lambda|b|^2 = a \tag{4.26}$$

Also since the total cost is

$$\int_0^1 |u|^2 dt = \lambda^2 |b|^2 \tag{4.27}$$

we see that the optimal choice of input is $\lambda = 2\pi$ and $|b|^2 = a/2\pi$ but otherwise is arbitrary. The structure of the optimal control for steering between the conjugate points $(0,0,0)$ and $(0,0,a)$ is interesting—it is sums of sines and cosines at a frequency of 2π. The frequency of the signal is dictated by the time interval. Note that the optimal input is still a combination of sines and cosines even if $x_1(1) \neq 0$ or $x_2(1) \neq 0$.

The generalization of this example to the case that $m > 2$ is as follows: consider the situation that the $\{b_i(x)\colon i = 1, \cdots, m\}$ are linearly independent for all x and also all the $m(m-1)$ first-order (first-*etage*) brackets $\{[b_i(x), b_j(x)]\colon i, j = 1, \cdots, m\}$ are linearly independent of the $b_i(x)$. The minimum dimension of the state space to allow for this possibility is $n = m + m(m-1)/2$. The canonic example of this situation is

$$\begin{aligned} \dot{x}_i &= u_i & i &= 1, \cdots, m \\ \dot{x}_{ij} &= x_i u_j - x_j u_i & i &= 1, \cdots, m \end{aligned} \tag{4.28}$$

A slightly more pleasing representation of equation (4.28) is obtained by forming the skew symmetric matrix $Y \in \mathbb{R}^{m \times m}$ with the x_{ij} as the bottom lower half (below the diagonal).

$$\dot{x} = u \tag{4.29}$$
$$\dot{Y} = xu^T - ux^T \tag{4.30}$$

The Euler-Lagrange equations for (4.28) are an extension of (4.22):

$$\ddot{x} = \Lambda\dot{x} \tag{4.31}$$
$$\dot{\Lambda} = 0 \tag{4.32}$$

where Λ is the skew symmetric $m \times m$ matrix of Lagrange multipliers associated with Y. Thus, as before, the optimal input u satisfies the equation

$$\dot{u} = \Lambda u \tag{4.33}$$

with $\Lambda \in \mathbb{R}^{m \times m}$ begin a constant, skew symmetric matrix. Thus $u(t)$ is a linear combination of sinusoids. The exact eigenvalues of Λ are determined by the initial and final state. In fact, if $x(0) = x(1) = 0$, $Y(0) = 0$ and $Y(1)$ a nonsingular $m \times m$ skew symmetric matrix (this requires that m is even), then it can be shown that Λ has $m/2$ sinusoids at frequencies 2π, $2 \cdot 2\pi$, $\cdots$, $m/2 \cdot 2\pi$. If m is odd and $Y(1)$ has only one zero eigenvalue, Λ has one zero eigenvalue and $(m-1)/2$ sinusoids at frequencies 2π, $2 \cdot 2\pi$, $\cdots$, $(m-1)/2 \cdot 2\pi$.

4.3 Steering of controllable systems

The results of the previous section derive the geodesics for first etage, linear systems of the form in equation (4.17). There are several ways of generalizing this further:

1. build model control systems where the vector fields

$$\begin{array}{ll} b_i & i = 1, \cdots, m \\ [b_i, b_j] & i, j = 1, \ldots, m \\ [[b_i, b_j], b_k] & i, j, k = 1, \cdots, m \end{array}$$

   are linearly independent and $n = m + m(m-1)/2 + m(m-1)(m+1)/3$.

2. understand conditions under which more general control systems can be transformed into canonical systems studied above.

3. use the results summarized thus far as inspiration to propose sinusoidal inputs at multiple frequencies which are integrally related to provide (sub-optimal) control laws to steer the systems between arbitrary initial and final conditions.

In this section we shall explore the latter possibility.

First Etage Controllable Systems

By *first etage controllable systems* we mean systems of the form (4.17) with $m < n$, with the columns of $B(x)$ linearly independent and with

$$\text{span}\{b_i(x),\ [b_i(x), b_j(x)] : i, j = 1, \ldots, m\} = \mathbb{R}^n \tag{4.34}$$

Namely, one level of Lie brackets is adequate to achieve the full tangent space for all x. We discussed the optimal control of canonical systems satisfying (4.34) in Section 4.1. Here we illustrate the application of this problem to the steering of a unicycle as shown in Figure 4.1. If u_1 denotes the driving velocity and u_2 the steering velocity the functional form of the state equations for this system is

$$\begin{aligned} \dot{x} &= \cos\phi\, u_1 \\ \dot{y} &= \sin\phi\, u_1 \\ \dot{\phi} &= u_2 \end{aligned} \tag{4.35}$$

An approximation to this system is obtained by setting $\cos\phi \simeq 1, \sin\phi \simeq \phi$ and relabelling x as x_1, y as x_3 and ϕ as x_2 to get

$$\begin{aligned} \dot{x}_1 &= u_1 \\ \dot{x}_2 &= u_2 \\ \dot{x}_3 &= x_2 u_1 \end{aligned} \tag{4.36}$$

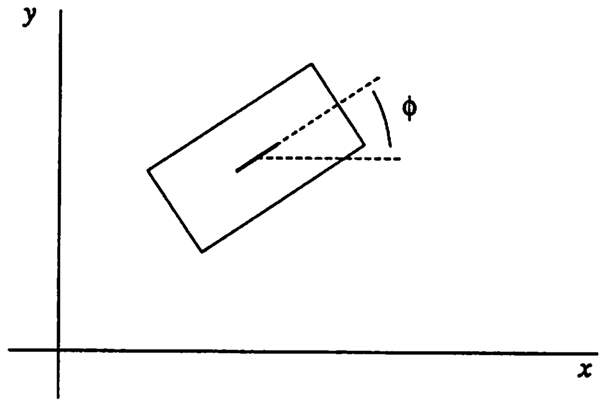

Figure 4.1: Steerable unicycle. The unicycle has two independent inputs: the *steering* input controls the angle of the wheel, ϕ; the *driving* input controls the velocity of the cart in the direction of the wheel. The configuration of the cart is its Cartesian location and the wheel angle.

To steer this system, we first use u_1, u_2 to steer x_1, x_2 to their desired locations; this may cause x_3 to drift. Now use $u_1 = \alpha \sin(\omega t), u_2 = \beta \cos(\omega t)$ and note that after $2\pi/\omega$ seconds, x_1 and x_2 complete a periodic trajectory and the x_3 coordinate advances by an amount equal to

$$\frac{\pi\alpha\beta}{\omega^2}$$

α, β, ω can now be chosen appropriately. In order to apply this strategy to the unapproximated system (4.35) we modify the input to

$$\begin{aligned} v_1 &= \cos\phi\, u_1 \\ v_2 &= u_2 \end{aligned}$$

and relabel the states to get

$$\begin{aligned} \dot{x}_1 &= v_1 \\ \dot{x}_2 &= v_2 \\ \dot{x}_3 &= \tan x_2\, v_1 \end{aligned} \tag{4.37}$$

As before, we steer x_1 and x_2 using v_1, v_2. To steer the third variable, we use $v_1 = \alpha \sin(\omega t), v_2 = \beta \cos(\omega t)$. Then

$$\dot{x}_3 = \tan(\frac{\beta}{\omega} \sin \omega t)\, \alpha \sin(\omega t) \tag{4.38}$$

The value of x_3 after $2\pi/\omega$ seconds is determined by the constant part of the right hand side of (4.38). The constant coefficient is given by

$$\frac{1}{2} \cdot \frac{1}{\pi} \int_{-\pi}^{\pi} \tan(\frac{\beta}{\omega} \sin\theta) \alpha \sin(\theta) d\theta$$

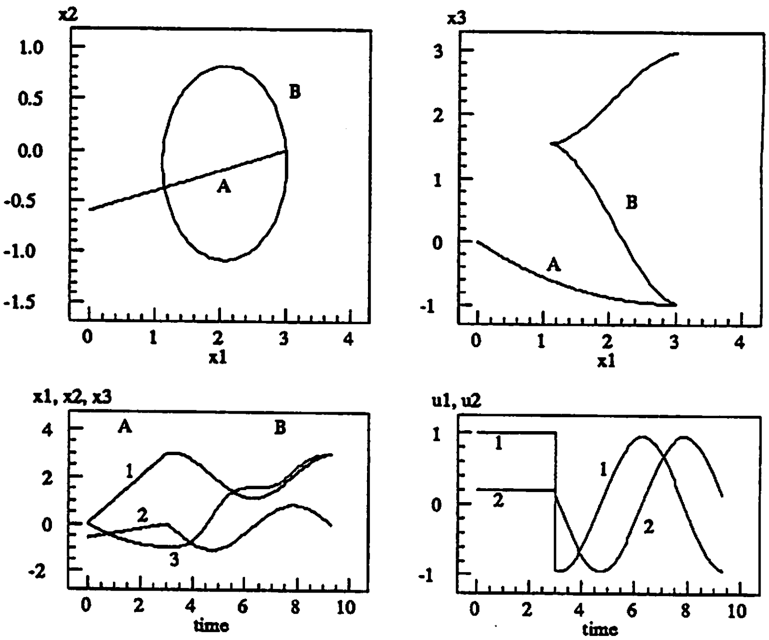

Figure 4.2: Sample Trajectories for the unicycle. The trajectory shown is a two stage path which moves the unicycle from (0, -.6, 0) to (3, 0, 3). The first portion of the path, labeled A, drives the x_1 and x_2 states to their desired values using a constant input. The second portion, labeled B, uses a periodic input to drive x_3 while bringing the other two states back to their desired values. The top two figures show the states versus x_1; the bottom figures show the states and inputs as functions of time.

Sample trajectories for this scenario are shown in Figure 4.2

Second and Higher Etage Controllable Systems

Systems (4.17) are said to be *second etage controllable* if

$$\mathrm{span}\{b_i(x),\ [b_i(x), b_j(x)],\ [b_i,[b_j,b_k]] : i,j,k = 1,\ldots,m\} = \mathbb{R}^n$$

An example of such a system is a front wheel drive cart of the form shown in Figure 4.3. As in the case of the previous example u_1 is the driving velocity and u_2 the steering velocity. The equations of this cart are

$$\begin{aligned} \dot{x} &= \cos\theta\cos\phi\, u_1 \\ \dot{y} &= \sin\theta\cos\phi\, u_1 \\ \dot{\phi} &= u_2 \\ \dot{\theta} &= \tfrac{1}{l}\sin\phi\, u_1 \end{aligned} \tag{4.39}$$

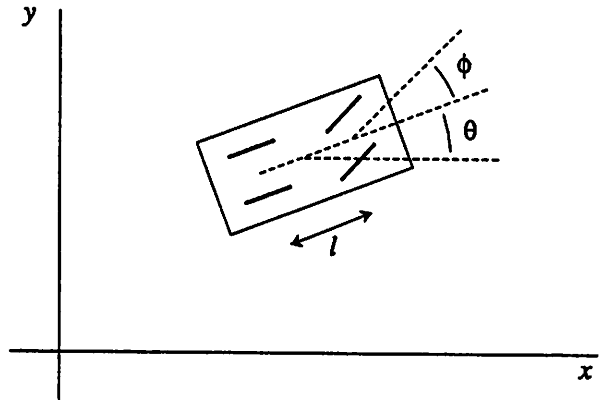

Figure 4.3: Front wheel drive cart. The configuration of the cart is determined by its Cartesian location, the angle the car makes with the horizontal and the steering wheel angle relative to the car body. The two inputs are the velocity of the front wheels (in the direction the wheels are pointing) and the steering velocity. The rear wheels of the cart are always aligned with the cart body and are constrained to move along the line in which they point or rotate about their center.

The form of the equations shows that when $\phi = \pi/2$, the cart cannot be driven forward. As in the previous section an approximation to this system is instructive. Relabelling the variables x, y, ϕ, θ as x_1, x_4, x_2, x_3, setting $l = 1$ and approximating sines and cosines as before yields

$$\begin{aligned} \dot{x}_1 &= u_1 \\ \dot{x}_2 &= u_2 \\ \dot{x}_3 &= x_2 u_1 \\ \dot{x}_4 &= x_3 u_1 \end{aligned} \tag{4.40}$$

Note that $\text{span}\{b_1, b_2, [b_1, b_2], [b_1, [b_1, b_2]]\} = \mathbf{R}^n$ so that system is a second etage system. It is also easy to verify that this condition also holds for the original system. Steering the states x_1, x_2, x_3 of (4.40) is immediate from the previous section. To steer x_4 note that if

$$u_1 = \alpha \cos \omega t \ , \ u_2 = \beta \cos 2\omega t$$

then x_1, x_2 and x_3 are all periodic and return to their initial values after $2\pi/\omega$ seconds. Also

$$x_3 = -\frac{\alpha\beta}{4\omega^2} \cos \omega t \ - \ \frac{\alpha\beta}{12\omega^2} \cos 3\omega t$$

so that it too is periodic. Finally the increment in x_4 is given by

$$-\frac{\pi \alpha^2 \beta}{4\omega^3}$$

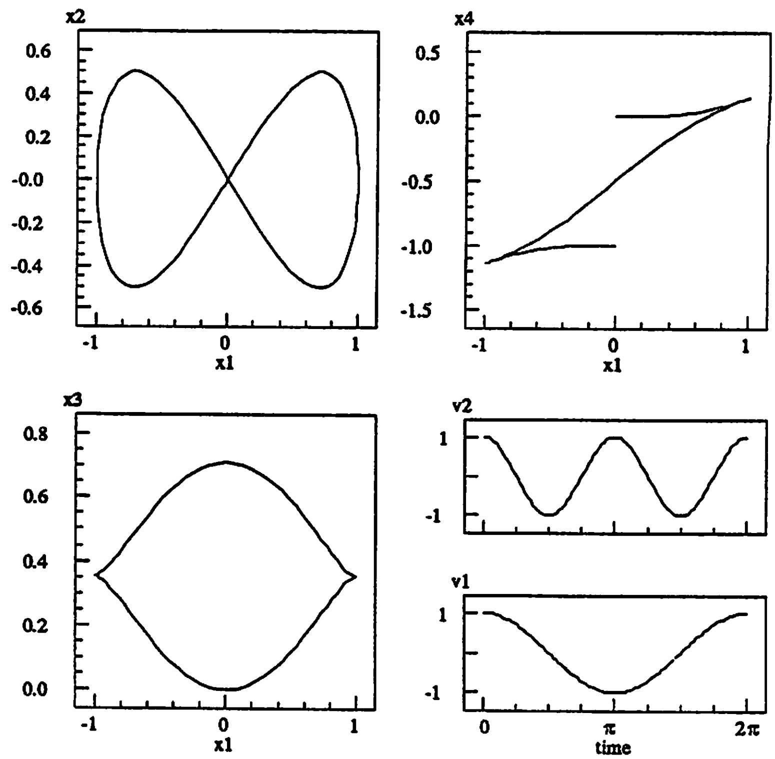

Figure 4.4: Trajectories for a simple cart. The trajectory shown illustrates motion in the x_4 direction. Periodic inputs are used to generate periodic trajectories in the first three states while giving an open trajectory in the last state.

To carry this development through for the unapproximated system define $v_1 = u_1 \cos\theta \cos\phi$ and $v_2 = u_2$. Then with the same relabelling as before, the equations become

$$\begin{aligned} \dot{x}_1 &= v_1 \\ \dot{x}_2 &= v_2 \\ \dot{x}_3 &= \frac{\tan(x_2)}{\cos(x_3)} v_1 \\ \dot{x}_4 &= \tan x_3 v_1 \end{aligned} \tag{4.41}$$

We refer to such systems as *triangular* but not *strictly triangular* since $\dot{x}_3$ depends on x_3. By approximating $\cos x_3$ by 1, the equations become strictly triangular; using $v_1 = \alpha \cos \omega t$, $v_2 = \beta \cos 2\omega t$ we can solve for the Fourier series coefficients of x_1, x_2, x_3 and x_4. Note that only the Fourier coefficient corresponding to the zero frequency is needed to get the change in x_4 after one time period.

To summarize, it is easy to see that for higher etage (than 2) controllable systems one can use simple Fourier series techniques to steer the systems using as inputs integrally related sinusoids provided that they are strictly triangular in the sense discussed above. To steer the variable corresponding to the k^{th} etage it is possible to use frequencies ω and $k\omega$ in the two inputs. The Lissajous figures that are obtained from the phase portraits of the different variables are quite instructive. Consider the Figure 4.4, which is the system of (4.41) with $\cos x_3$ replaced by 1 and the inputs $v_1 = \alpha \cos \omega t$, $v_2 = \beta \cos 2\omega t$. The upper left plot is the Lissajous figure for x_1, x_2 (two loops); The lower left plot is the corresponding figure for x_3, x_1 (one loop) and the open curve in x_4,x_1 shows the increment in the x_4 variable. The very powerful implication here is that the *Lie bracket directions correspond to rectification of harmonic periodic motions of the driving vector fields and the harmonic relations are determined by the etage of controllability desired.* This point has also been made rather elegantly by Brockett [3] in the context of the rectification of mechanical motion.

Open Problems and Nontriangular Higher Etage Systems

Consider the kinematic equations for a front wheel drive cart with a trailer as shown in Figure 4.5. The kinematic equations are those of the car with an additional equation to describe the angle of the trailer:

$$
\begin{aligned}
\dot{x} &= \cos\theta \cos\phi \, u_1 \\
\dot{y} &= \sin\theta \cos\phi \, u_1 \\
\dot{\theta} &= \tfrac{1}{l} \sin\phi \, u_1 \\
\dot{\phi} &= u_2 \\
\dot{\psi} &= \tfrac{1}{d} \sin(\theta - \psi) \cos\phi \, u_1
\end{aligned}
\tag{4.42}
$$

It may be verified that

$$
\mathrm{span}\{b_1,\ b_2,\ [b_1, b_2],\ [b_1,[b_1,b_2]],\ [b_1,[b_1,[b_1,b_2]]]\} = \mathbb{R}^5
$$

It is also not difficult to see that with k trailers we need Lie brackets up to the $k{+}2$ etage to guarantee controllability. Also, it may be seen that after redefining the inputs the system is only triangular rather than strictly triangular so that the harmonic analysis techniques of the previous section cannot be applied even though numerical simulation suggests that sinusoids of integer multiples are useful to steer along the direction of the j^{th} Lie bracket. The full theory for these systems is as yet incomplete.

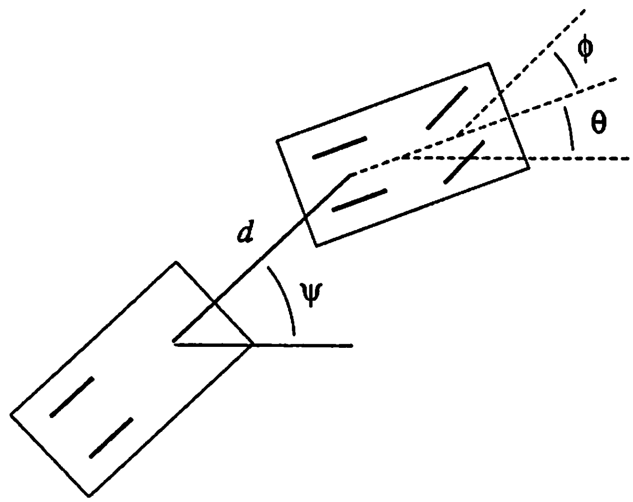

Figure 4.5: Front wheel drive cart with trailer. The trailer configuration is described the the angle the trailer makes with the horizontal, ψ. The rear wheels of the trailer are fixed and constrained to move along the line in which they point or rotate about their center. The inputs to the system are the inputs to the cart: the driving velocity (of the front wheels) and the steering velocity. This system is an example of a third etage system; higher etage systems can be generated by adding extra trailers.

4.4 Dynamic finger repositioning revisited

We now reconsider the case of a multifingered hand grasping an object. The equations of motion are given by equation (4.14) which we reproduce here:

$$\begin{aligned} \dot{x}_o &= u_1 \\ \dot{\eta} &= B_1(x_o, \eta)u_1 + B_2(x_o, \eta)u_2 \end{aligned} \tag{4.43}$$

Recall that these equations were obtained by attaching a controller to the system and letting u_1 reflect the desired object velocity and u_2 parameterize the internal motion of the system.

The general case of finding $u_1(t)$ and $u_2(t)$ such that the object and the fingers move from an initial to final position (while maintaining contact) can be very difficult. $B_1(x_o, \eta)$ and $B_2(x_o, \eta)$ are rarely in any of the simple forms that we have considered thus far. We point out two interesting special cases:

1. If the hand has no redundant degrees of freedom (i.e., B_2 is not present) then it might be possible to move to an arbitrary location/grasp using only u_1. Moving just the contact location requires a carefully chosen closed loop path in x_o.

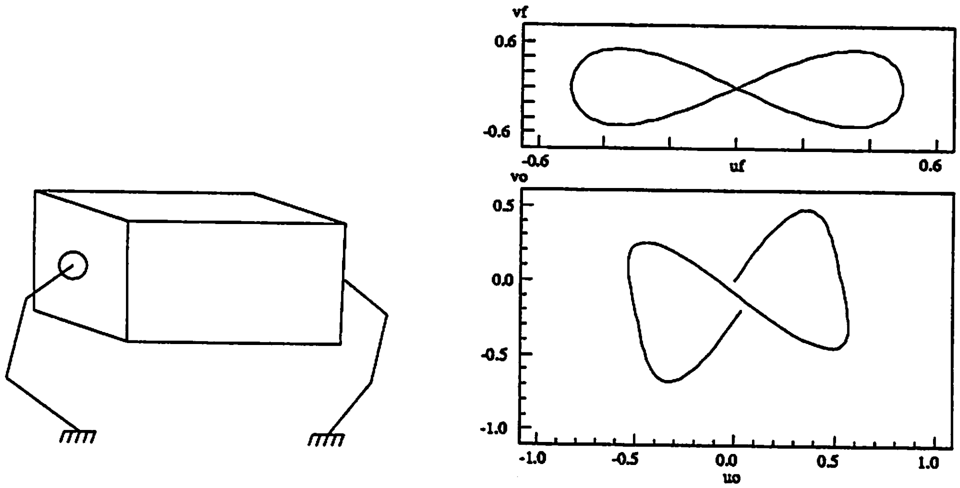

Figure 4.6: Steering applied to a multifingered hand. We consider the motion of a finger with a spherical tip on a polyhedral object (left). The plots to the right show a trajectories which move a finger down the side of an object. The location of the contact on the finger is unchanged (upper graph), while the location of the contact on the face of the object undergoes a net y displacement (lower graph).

2. If we have redundant degrees of freedom, then we can move the fingers along the object while keeping the object position fixed ($\dot{x}_o = u_1 = 0$). In this case we use only the vector fields in B_2 to move the fingers.

In the second case, it is sufficient to study the control of a single finger since the fingers are decoupled if the object is held fixed. This situation has been studied by Li and Canny [9] and we review some examples from that paper in the context of steering controllable systems.

Examples

Consider the case of a single spherical finger rolling on a plane. The control kinematics were derived in Section 2.3:

$$\dot{\eta} = \begin{pmatrix} \dot{u}_f \\ \dot{v}_f \\ \dot{u}_o \\ \dot{v}_o \\ \dot{\psi} \end{pmatrix} = \begin{pmatrix} 1 \\ 0 \\ \rho\cos\psi \\ -\rho\sin\psi \\ 0 \end{pmatrix} \omega_1 + \begin{pmatrix} 0 \\ \sec u_f \\ -\rho\sin\psi \\ -\rho\cos\psi \\ -\tan u_f \end{pmatrix} \omega_2 \tag{4.44}$$

For simplicity, we assume that we control ω_1 and ω_2 directly. It can be verified that the system is second etage controllable and that by a change of input variables we can put this system into strictly triangular form. Furthermore, the approximate version of this system is given by

$$\begin{array}{rrcl} u_f: & \dot{x}_1 & = & u_1 \\ v_f: & \dot{x}_2 & = & u_2 \\ -\psi: & \dot{x}_3 & = & x_1 u_2 \\ u_o - \rho u_f: & \dot{x}_4 & = & x_3 u_2 \\ v_o + \rho v_f: & \dot{x}_5 & = & x_3 u_1 \end{array} \tag{4.45}$$

This is identical to the approximat cart kinematics in equation (4.40) with the addition of an extra state. Using the same techniques as before, we can construct paths using integrally related sinusoids and apply these sinusoids to the full nonlinear system in equation (4.44). An example of a path which moves a finger vertically down the side of a planar object is shown in Figure 4.6.

A more challenging example considered by Li and Canny is that of moving a spherical finger on a spherical object. It may be verified that the system is controllable except when the object and finger radii are identical (in this case the rolling constraint becomes holonomic). The contact kinematics, from equation (2.43) are

$$\dot{\eta} = \begin{pmatrix} \frac{1}{1+\rho} \\ 0 \\ \frac{\rho}{1+\rho}\cos\psi \\ -\frac{\rho}{1+\rho}\sin\psi\sec u_o \\ \frac{\rho}{1+\rho}\sin\psi\tan u_o \end{pmatrix} \omega_1 + \begin{pmatrix} 0 \\ \frac{1}{1+\rho}\sec u_f \\ -\frac{\rho}{1+\rho}\sin\psi \\ -\frac{\rho}{1+\rho}\cos\psi\sec u_o \\ \frac{\rho}{1+\rho}(\cos\psi\tan u_o - 1/\rho\ \tan u_f) \end{pmatrix} \omega_2 \tag{4.46}$$

We see that this system is not strictly triangular (ψ depends on u_o) and hence requires a more sophisticated approach. Motion for this particular system can be constructed using the techniques described by Li and Canny due to the special choice of object and finger shapes. Motion planning for more general choices of finger and object shapes is still unsolved.

Acknowledgements

We would like to thank Roger Brockett for introducing us to his work on singular Riemannian metrics (Chapter 4), Li Zexiang for making the connections between regrasping and steering, and John Canny, Jean-Paul Laumond and the denizens of the robotics lab for several useful discussions.

Bibliography

[1] A. K. Bejczy. Robot arm dynamics and control. Technical Report 33-699, Jet Propulsion Laboratory, 1974.

[2] R. W. Brockett. Control theory and singular riemannian geometry. In *New Directions in Applied Mathematics*, pages 11–27. Springer-Verlag, New York, 1981.

[3] R. W. Brockett. On the rectification of vibratory motion. *Sensors and Actuators*, 1989. (to appear).

[4] A. Cole, J. Hauser, and S. Sastry. Kinematics and control of multifingered hands with rolling contact. In *IEEE International Conference on Robotics and Automation*, pages 228–233, 1988.

[5] J. Kerr. *An Analysis of Multi-fingered Hands*. PhD thesis, Stanford University, Department of Mechanical Engineering, 1984.

[6] O. Khatib. A unified approach for motion and force control of robot manipulators: The operational space formulation. *IEEE Journal on Robotics and Automation*, RA-3(1):43–53, 1987.

[7] O. Khatib. Augmented object and reduced effective inertia in robot systems. In *Automatic Control Conference*, 1988.

[8] D. Koditschek. Natural motion for robot arms. In *IEEE Control and Decision Conference*, pages 733–735, 1984.

[9] Z. Li and J. Canny. Motion of two rigid bodies with rolling constraint. *IEEE Transactions on Robotics and Automation*, 6(1):62–71, 1990.

[10] Z. Li, P. Hsu, and S. Sastry. On kinematics and control of multifingered hands. In *IEEE International Conference on Robotics and Automation*, pages 384–389, 1988.

[11] J. Y. S. Luh, M. W. Walker, and R. P. Paul. Resolved acceleration control of mechanical manipulators. *IEEE Transactions on Automatic Control*, AC-25, 1980.

[12] D. J. Montana. The kinematics of contact and grasp. *International Journal of Robotics Research*, 7(3):17–32, 1988.

[13] R. Murray and S. Sastry. Control experiments in planar manipulation and grasping. In *IEEE International Conference on Robotics and Automation*, pages 624–631, 1989.

[14] V-D. Nguyen. Constructing force-closure grasps. *International Journal of Robotics Research*, 7(3):3–16, 1988.

[15] R. M. Rosenberg. *Analytical Dynamics of Discrete Systems*. Plenum Press, New York, 1977.

[16] N. Sadegh. *Adaptive Control of Mechanical Manipulators: Stability and Robustness Analysis*. PhD thesis, Department of Mechanical Engineering, University of California, Berkeley, California, 1987.

[17] J. E. Slotine and W. Li. On the adaptive control of robot manipulators. *International Journal of Robotics Research*, 6:49–59, 1987.